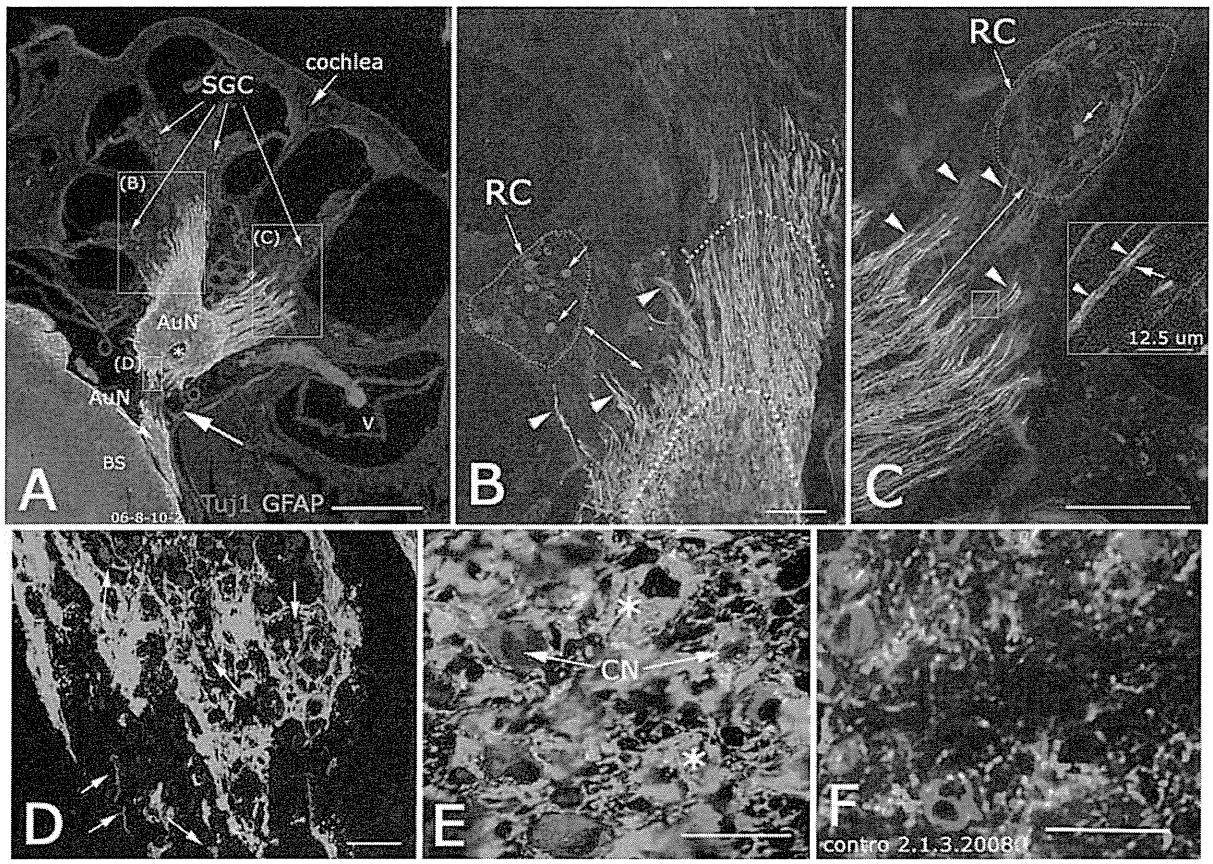

FIG. 12. Morphological changes in the auditory nervous system 8 weeks after compression in a Group B rat (the same animal as in Fig. 11). Extensive astrocytic outgrowth from the TZ was evident (**A–C**). The length of many astrocytic processes was more than 300 μm from the TZ (*dotted lines* in **B**). In the basal turn of the cochlea where the astrocytic outgrowth was greatest, the elongated processes occupied all the orifices of the TSF (*arrowheads* in **C**). The rectangle in C is enlarged in the **inset**; the astrocytic processes (indicated by *arrowheads*) ran parallel with the residual auditory neurons (indicated by *arrow*). In the lesion epicenter, dense plexiform gliotic tissue surrounded neural tissue fragments (*arrows* in **D**). Multiple, small areas unlabeled for GFAP were observed at the compressed site (*asterisk* in A). In the cochlear nucleus, neurons were surrounded by dense gliotic tissue (*asterisks* in E; cochlear nucleus region in control, F). The transverse diameter of the auditory nerve at and proximal to the compression site was reduced in comparison with that in the Group A rats at 8 weeks postcompression (Fig. 8). The *small arrows* in the Rosenthal canals in **B and C** indicate the residual spiral ganglion cells after compression. Anti-GFAP and anti–beta III-tubulin (clone Tuj1) immunostaining. Bar = 500 μm (A), 100 μm (B), 200 μm (C), 25 μm (D), 25 μm (E), and 25 μm (F).

References

1. Abe H, Rhoton AL Jr: Microsurgical anatomy of the cochlear nuclei. **Neurosurgery 58:**728–739, 2006
2. Asai Y, Umemura K, Nakashima M: Reversibility of compound action potential during the acute phase after transitory local ischemia. **Ann Otol Rhinol Laryngol 105:**472–475, 1996
3. Badie B, Pyle GM, Nguyen PH, Hadar EJ: Elevation of internal auditory canal pressure by vestibular schwannomas. **Otol Neurotol 22:**696–700, 2001
4. Bechmann I, Nitsch R: Astrocytes and microglial cells incorporate degenerating fibers following entorhinal lesion: a light, confocal, and electron microscopical study using a phagocytosis-dependent labeling technique. **Glia 20:**145–154, 1997
5. Betchen SA, Walsh J, Post KD: Long-term hearing preservation after surgery for vestibular schwannoma. **J Neurosurg 102:**6–9, 2005
6. Buffo A, Rite I, Tripathi P, Lepier A, Colak D, Horn AP, et al: Origin and progeny of reactive gliosis: A source of multipotent cells in the injured brain. **Proc Natl Acad Sci U S A 105:**3581–3586, 2008
7. Burnett MG, Zager EL: Pathophysiology of peripheral nerve injury: a brief review. **Neurosurg Focus 16(5):**E1, 2004
8. Campos-Torres A, Touret M, Vidal PP, Barnum S, de Waele C: The differential response of astrocytes within the vestibular and cochlear nuclei following unilateral labyrinthectomy or vestibular afferent activity blockade by transtympanic tetrodotoxin injection in the rat. **Neuroscience 130:**853–865, 2005
9. Chee GH, Nedzelski JM, Rowed D: Acoustic neuroma surgery: the results of long-term hearing preservation. **Otol Neurotol 24:**672–676, 2003
10. Cheng HW, Jiang T, Brown SA, Pasinetti GM, Finch CE, McNeill TH: Response of striatal astrocytes to neuronal deafferentation: an immunocytochemical and ultrastructural study. **Neuroscience 62:**425–439, 1994
11. Chiappa KH: Brain stem auditory evoked potentials: methodology, in Chiappa KH (ed): **Evoked Potentials in Clinical Medicine, ed 2.** New York: Raven Press, 1990, pp 173–221

12. de Waele C, Campos Torres A, Josset P, Vidal PP: Evidence for reactive astrocytes in rat vestibular and cochlear nuclei following unilateral inner ear lesion. **Eur J Neurosci 8:**2006–2018, 1996
13. Eng LF, Ghirnikar RS, Lee YL: Glial fibrillary acidic protein: GFAP-thirty-one years (1969–2000). **Neurochem Res 25:**1439–1451, 2000
14. Eriksson NP, Persson JK, Svensson M, Arvidsson J, Molander C, Aldskogius H: A quantitative analysis of the microglial cell reaction in central primary sensory projection territories following peripheral nerve injury in the adult rat. **Exp Brain Res 96:**19–27, 1993
15. Fraher JP, Delanty FJ: The development of the central-peripheral transitional zone of the rat cochlear nerve. A light microscopic study. **J Anat 155:**109–118, 1987
16. Garrison CJ, Dougherty PM, Kajander KC, Carlton SM: Staining of glial fibrillary acidic protein (GFAP) in lumbar spinal cord increases following a sciatic nerve constriction injury. **Brain Res 565:**1–7, 1991
17. Gentschev T, Sotelo C: Degenerative patterns in the ventral cochlear nucleus of the rat after primary deafferentation. An ultra-structural study. **Brain Res 62:**37–60, 1973
18. Goel A, Sekhar LN, Langheinrich W, Kamerer D, Hirsch B: Late course of preserved hearing and tinnitus after acoustic neurilemoma surgery. **J Neurosurg 77:**685–689, 1992
19. Graeber MB, Kreutzberg GW: Astrocytes increase in glial fibrillary acidic protein during retrograde changes of facial motor neurons. **J Neurocytol 15:**363–373, 1986
20. Johnsson LG, Hawkins JE Jr, Rouse RC: Sensorineural and vascular changes in an ear with acoustic neurinoma. **Am J Otolaryngol 5:**49–59, 1984
21. Julow J, Szeifert GT, Bálint K, Nyáry I, Nemes Z: The role of microglia/macrophage system in the tissue response to I-125 interstitial brachytherapy of cerebral gliomas. **Neurol Res 29:**233–238, 2007
22. Kakulas BA: The applied neuropathology of human spinal cord injury. **Spinal Cord 37:**79–88, 1999
23. Kapadia SE, LaMotte CC: Deafferentation-induced alterations in the rat dorsal horn: I. Comparison of peripheral nerve injury vs. rhizotomy effects on presynaptic, postsynaptic, and glial processes. **J Comp Neurol 266:**183–197, 1987
24. Koos W, Perneczky A: Suboccipital approach to acoustic neurinomas with emphasis on preservation of facial nerve and cochlear nerve function, in Rand RW (ed): **Microneurosurgery, ed 3.** St. Louis: CV Mosby, 1985, pp 335–365
25. Kountakis SE, Maillard AA, Urso R, Stiernberg CM: Endoscopic approach to traumatic visual loss. **Otolaryngol Head Neck Surg 116:**652–655, 1997
26. Lang J Jr, Ohmachi N, Lang J Sr: Anatomical landmarks of the Rhomboid fossa (floor of the 4th ventricle), its length and its width. **Acta Neurochir (Wien) 113:**84–90, 1991
27. Lapsiwala SB, Pyle GM, Kaemmerle AW, Sasse FJ, Badie B: Correlation between auditory function and internal auditory canal pressure in patients with vestibular schwannomas. **J Neurosurg 96:**872–876, 2002
28. Liu L, Rudin M, Kozlova EN: Glial cell proliferation in the spinal cord after dorsal rhizotomy or sciatic nerve transection in the adult rat. **Exp Brain Res 131:**64–73, 2000
29. Liu PH, Yang LH, Wang TY, Wang YJ, Tseng GF: Proximity of lesioning determines response of facial motoneurons to peripheral axotomy. **J Neurotrauma 23:**1857–1873, 2006
30. Matsumoto M, Sekiya T, Kojima K, Ito J: An animal experimental model of auditory neuropathy induced in rats by auditory nerve compression. **Exp Neurol 210:**248–256, 2008
31. Matthies C, Thomas S, Moshrefi M, Lesinski-Schiedat A, Frohne C, Battmer RD, et al: Auditory brainstem implants: current neurosurgical experiences and perspective. **J Laryngol Otol Suppl 27:**32–36, 2000
32. McKenna MJ, Halpin C, Ojemann RG, Nadol JB Jr, Montgomery WW, Levine RA, et al: Long-term hearing results in patients after surgical removal of acoustic tumors with hearing preservation. **Am J Otol 13:**134–136, 1992
33. Møller AR, Burgess J: Neural generators of the brain-stem auditory evoked potentials (BAEPs) in the rhesus monkey. **Electroencephalogr Clin Neurophysiol 65:**361–372, 1986
34. Møller AR, Jannetta P, Bennett M, Møller MB: Intracranially recorded responses from the human auditory nerve: new insights into the origin of brain stem evoked potentials (BSEPs). **Electroencephalogr Clin Neurophysiol 52:**18–27, 1981
35. Morest DK, Kim J, Potashner SJ, Bohne BA: Long-term degeneration in the cochlear nerve and cochlear nucleus of the adult chinchilla following acoustic overstimulation. **Microsc Res Tech 41:**205–216, 1998
36. Moriyama T, Fukushima T, Asaoka K, Roche PH, Barrs DM, McElveen JT Jr: Hearing preservation in acoustic neuroma surgery: importance of adhesion between the cochlear nerve and the tumor. **J Neurosurg 97:**337–340, 2002
37. Müller M: Frequency representation in the rat cochlea. **Hear Res 51:**247–254, 1991
38. Pekny M: Astrocytic intermediate filaments: lessons from GFAP and vimentin knock-out mice. **Prog Brain Res 132:** 23–30, 2001
39. Pekny M, Wilhelmsson U, Bogestål YR, Pekna M: The role of astrocytes and complement system in neural plasticity. **Int Rev Neurobiol 82:**95–111, 2007
40. Perlman HB, Kimura R, Fernandez C: Experiments on temporary obstruction of the internal auditory artery. **Laryngoscope 69:**591–613, 1959
41. Ridet JL, Malhotra SK, Privat A, Gage FH: Reactive astrocytes: cellular and molecular cues to biological function. **Trends Neurosci 20:**570–577, 1997
42. Salvador-Silva M, Vidal-Sanz M, Villegas-Pérez MP: Microglial cells in the retina of Carassius auratus: effects of optic nerve crush. **J Comp Neurol 417:**431–447, 2000
43. Sekiya T, Hatayama T, Shimamura N, Suzuki S: An in vivo quantifiable model of cochlear neuronal degeneration induced by central process injury. **Exp Neurol 161:**490–502, 2000
44. Sekiya T, Kojima K, Matsumoto M, Holley MC, Ito J: Rebuilding lost hearing using cell transplantation. **Neurosurgery 60:**417–433, 2007
45. Sekiya T, Møller AR: Cochlear nerve injuries caused by cerebellopontine angle manipulations. An electrophysiological and morphological study in dogs. **J Neurosurg 67:**244–249, 1987
46. Shaw NA: The auditory evoked potential in the rat—a review. **Prog Neurobiol 31:**19–45, 1988
47. Shelton C, Hitselberger WE, House WF, Brackmann DE: Hearing preservation after acoustic tumor removal: long-term results. **Laryngoscope 100:**115–119, 1990
48. Shortland P, Woolf CJ: Chronic peripheral nerve section results in a rearrangement of the central axonal arborizations of axotomized A beta primary afferent neurons in the rat spinal cord. **J Comp Neurol 330:**65–82, 1993
49. Stensaas LJ, Partlow LM, Burgess PR, Horch KW: Inhibition of regeneration: the ultrastructure of reactive astrocytes and abortive axon terminals in the transition zone of the dorsal root. **Prog Brain Res 71:**457–468, 1987
50. Stjernholm C, Muren C: Dimensions of the cochlear nerve canal: a radioanatomic investigation. **Acta Otolaryngol 122:** 43–48, 2002
51. Strauss C, Bischoff B, Romstöck J, Rachinger J, Rampp S, Prell J: Hearing preservation in medial vestibular schwannomas. **J Neurosurg 109:**70–76, 2008
52. Sumner BE, Sutherland FI: Quantitative electron microscopy on the injured hypoglossal nucleus in the rat. **J Neurocytol 2:**315–328, 1973
53. Tarlov IM: Structure of the nerve root. II. Differentiation of sensory from motor roots: observations on identification of

function in roots of mixed cranial nerves. **Arch Neurol Psychiatry 37:**1338–1355, 1937
54. Tatagiba M, Matthies C, Samii M: Microendoscopy of the internal auditory canal in vestibular schwannoma surgery. **Neurosurgery 38:**737–740, 1996
55. Tator CH: Review of treatment trials in human spinal cord injury: issues, difficulties, and recommendations. **Neurosurgery 59:**957–987, 2006
56. Tetzlaff W, Graeber MB, Bisby MA, Kreutzberg GW: Increased glial fibrillary acidic protein synthesis in astrocytes during retrograde reaction of the rat facial nucleus. **Glia 1:**90–95, 1988
57. Totoiu MO, Keirstead HS: Spinal cord injury is accompanied by chronic progressive demyelination. **J Comp Neurol 486:**373–383, 2005
58. Tucci DL, Telian SA, Kileny PR, Hoff JT, Kemink JL: Stability of hearing preservation following acoustic neuroma surgery. **Am J Otol 15:**183–188, 1994
59. Umezu H, Aiba T, Tsuchida S, Seki Y: Early and late postoperative hearing preservation in patients with acoustic neuromas. **Neurosurgery 39:**267–272, 1996
60. Viberg A, Canlon B: The guide to plotting a cochleogram. **Hear Res 197:**1–10, 2004
61. Yong RL, Westerberg BD, Dong C, Akagami R: Length of tumor-cochlear nerve contact and hearing outcome after surgery for vestibular schwannoma. **J Neurosurg 108:**105–110, 2008

Manuscript submitted December 6, 2009.
Accepted February 16, 2010.
Please include this information when citing this paper: published online April 2, 2010; DOI: 10.3171/2010.2.JNS091817.
Address correspondence to: Tetsuji Sekiya, M.D., Department of Otolaryngology, Head and Neck Surgery, Kyoto University Graduate School of Medicine, Sakyou-ku, Kyoto, 606-8507 Japan. email: tsekiya@ent.kuhp.kyoto-u.ac.jp.

Hearing Research 270 (2010) 110–118

Contents lists available at ScienceDirect

Hearing Research

journal homepage: www.elsevier.com/locate/heares

Research paper

Salicylate restores transport function and anion exchanger activity of missense pendrin mutations

Kenji Ishihara [a,b], Shuhei Okuyama [a], Shun Kumano [a], Koji Iida [a], Hiroshi Hamana [a], Michio Murakoshi [a], Toshimitsu Kobayashi [c], Shinichi Usami [d], Katsuhisa Ikeda [e], Yoichi Haga [f], Kohei Tsumoto [g], Hiroyuki Nakamura [h], Noriyasu Hirasawa [i], Hiroshi Wada [a,*]

[a] *Department of Bioengineering and Robotics, Graduate School of Engineering, Tohoku University, 6-6-01, Aoba, Aramaki, Aoba-ku, Sendai, Miyagi 980-8579, Japan*
[b] *Laboratory of Medical Science, Course for School Nurse Teacher, Faculty of Education, Ibaraki University, 310-8512, Japan*
[c] *Department of Otolaryngology Head and Neck Surgery, Graduate School of Medicine, Tohoku University, 980-8575, Japan*
[d] *Department of Otorhinolaryngology, Shinshu University School of Medicine, 390-8621, Japan*
[e] *Department of Otorhinolaryngology, Juntendo University School of Medicine, 113-8421, Japan*
[f] *Department of Biomedical Engineering, Graduate School of Biomedical Engineering, Tohoku University, 980-8579, Japan*
[g] *Department of Medical Genome Sciences, Graduate School of Frontier Sciences, The University of Tokyo, 277-8562, Japan*
[h] *Department of Chemistry, Faculty of Science, Gakusyuin University, 171-8588, Japan*
[i] *Laboratory of Pharmacotherapy of Life-Style Related Diseases, Graduate School of Pharmaceutical Sciences, Tohoku University, 980-8578, Japan*

ARTICLE INFO

Article history:
Received 15 April 2010
Received in revised form
26 August 2010
Accepted 30 August 2010
Available online 6 September 2010

ABSTRACT

The *SLC26A4* gene encodes the transmembrane protein pendrin, which is involved in the homeostasis of the ion concentration of the endolymph of the inner ear, most likely by acting as a chloride/bicarbonate transporter. Mutations in the *SLC26A4* gene cause sensorineuronal hearing loss. However, the mechanisms responsible for such loss have remained unknown. Therefore, in this study, we focused on the function of ten missense pendrin mutations (p.P123S (Pendred syndrome), p.M147V (NSEVA), p.K369E (NSEVA), p.A372V (Pendred syndrome/NSEVA), p.N392Y (Pendred syndrome), p.C565Y (NSEVA), p.S657N (NSEVA), p.S666F (NSEVA), p.T721M (NSEVA) and p.H723R (Pendred syndrome/NSEVA)) reported in Japanese patients, and analyzed their cellular localization and anion exchanger activity using HEK293 cells transfected with each mutant gene. Immunofluorescent staining of the cellular localization of the pendrin mutants revealed that p.K369E and p.C565Y, as well as wild-type pendrin, were transported to the plasma membrane, while 8 other mutants were retained in the cytoplasm. Furthermore, we analyzed whether salicylate, as a pharmacological chaperone, restores normal plasma membrane localization of 8 pendrin mutants retained in the cytoplasm to the plasma membrane. Incubation with 10 mM of salicylate of the cells transfected with the mutants induced the transport of 4 pendrin mutants (p.P123S, p.M147V, p.S657Y and p.H723R) from the cytoplasm to the plasma membrane and restored the anion exchanger activity. These findings suggest that salicylate might contribute to development of a new method of medical treatment for sensorineuronal hearing loss caused by the mutation of the deafness-related proteins, including pendrin.

1. Introduction

The auditory system consists of three parts: the outer ear, middle ear and inner ear. Pendrin, which is encoded by the *PDS* (*SLC26A4*) gene, is a 780 amino acid, an 85.7 kDa membrane protein having 12 putative transmembrane domains, and is mainly expressed in the inner ear, thyroid gland and kidney (Everett et al., 1997). In the inner ear, pendrin is detected in the apical membrane of the endolymphatic duct, endolymphatic sac and various cells which compose the cochlea (Yoshino et al., 2004). Pendrin belongs to the *solute carrier 26A* (*SLC26A*) family, which is a group of proteins acting as multifunctional anion exchangers, and transports anions of Cl^-, I^-, $HCO3^-$ and formate (Scott et al., 1999; Mount and Romero, 2004; Wangemann et al., 2007; Kopp et al., 2008). Pendrin is thought to play an important role in the inner ear as a $Cl^-/HCO3^-$

Abbreviations: 7-AAD, 7-amino-actinomycin D; NASEVA, non-syndromic hearing loss with enlarged vestibular aqueduct; SLC26A, solute carrier 26A.

* Corresponding author. Tel.: +81 22 795 6938; fax: +81 22 795 6939.
E-mail address: wada@cc.mech.tohoku.ac.jp (H. Wada).

0378-5955/$ – see front matter © 2010 Elsevier B.V. All rights reserved.
doi:10.1016/j.heares.2010.08.015

transporter involved in the conditioning of ion concentration of the endolymphatic fluid (Mount and Romero, 2004; Wangemann et al., 2007). The loss of pendrin in *Slc26A4*$^{-/-}$ mice, which is a model for Pendred syndrome, results in failure of $HCO3^-$ secretion into endolymph, leading to hearing loss via acidification of endolymph and inhibition of Ca^{2+} reabsorption (Royaux et al., 2001; Wangemann et al., 2007).

More than 150 different mutations of the *PDS* gene have been found in humans so far. These mutations are responsible for Pendred syndrome, which is an autosomal recessive disorder characterized by sensorineuronal hearing loss, goiter and a partial defect in iodide organification, and for non-syndromic hearing loss with an enlarged vestibular aqueduct (NSEVA) (Everett et al., 1997; Kopp, 1999; Dossena et al., 2009). In Japanese, 18 point mutations of the *PDS* gene, i.e., 10 missense mutations, one stop mutation, four frameshift mutations, and three splice site mutations, are reported to lead to these disorders (Tsukamoto et al., 2003). Although Pendred syndrome is thought to account for up to 10% of all cases of syndromic hearing loss, no effective therapy for this syndrome has been established.

Abnormal protein folding or trafficking is associated with various diseases (Thomas et al., 1995; Taubes, 1996; Welch and Brown, 1996). Although, in general, newly synthesized membrane-associated and secreted proteins are translocated to the endoplasmic reticulum, where folding is facilitated by interaction of various endogenous chaperons, abnormal proteins produced by missense mutations are retained in the endoplasmic reticulum by misfolding (Ulloa-Aguirre et al., 2004). It is suggested that such retention and defective plasma membrane targeting of pendrin mutants play a key role in the pathogenesis of Pendred syndrome (Rotman-Pikielny et al., 2002; Dossena et al., 2009). Pharmacological rescue is one method of salvaging these defective proteins by low molecular compounds such as IN3 as chaperones (Conn et al., 2002; Ulloa-Aguirre et al., 2004). Pharmacological chaperones correct errors in folding and restore activity by reestablishing correct protein routing (Ulloa-Aguirre et al., 2004). It has been reported that the misfolded mutants of membrane proteins such as V2 vasopressin receptor, P-glycoprotein and GnRH receptor can be rescued by this method (Loo and Clarke, 1997; Morello et al., 2000; Janovick et al., 2002). Therefore, it is possible that recovery of pendrin mutants by some compounds could improve the condition of Pendred syndrome and NSEVA.

Recently, we have reported that salicylate, which binds to prestin with high affinity (Tunstall et al., 1995; Kakehata and Santos-Sacchi, 1996), induces the translocation of prestin mutants to the plasma membrane from the cytoplasm (Kumano et al., 2010). Prestin is a member of the *SLC26A* gene family including pendrin, and there is approximately a 45% similarity between these proteins in amino acid sequences. Therefore, we hypothesized that pendrin mutants retained in the cytoplasm are induced to translocate to the plasma membrane by salicylate and the function is restored.

In this study, we focused on the 10 missense pendrin mutations (p.P123S (Pendred syndrome), p.M147V (NSEVA), p.K369E (NSEVA), p.A372V (Pendred syndrome/NSEVA), p.N392Y (Pendred syndrome), p.C565Y (NSEVA), p.S657N (NSEVA), p.S666F (NSEVA), p.T721M (NSEVA) and p.H723R (Pendred syndrome/NSEVA)) found in Japanese patients (Tsukamoto et al., 2003) and analyzed the localization and anion transporter activity of these mutant proteins *in vitro* and the effects of salicylate as a pharmacological chaperone for the rescue of the pendrin mutants.

2. Methods

2.1. Construction of expression vectors

The sequences encoding an N-terminal FLAG tag were added by PCR amplification to the cDNA for human wild-type pendrin (Accession No. NM_000441.1) and the resulting insert was cloned into pcDNA3.1 (Invitrogen, Carlsbad, CA). *E. coli* JM109 was transformed with the constructed expression vector (pcDNA3.1/pendrin-FLAG). Mutational studies targeted the genes of pendrin missense mutations reported in Japanese patients (Tsukamoto et al., 2003). To express 10 pendrin mutants, the mutations were introduced into the pcDNA3.1/pendrin-FLAG using the primer sets shown in Table 1 and QuikChange II Site-Directed Mutagenesis Kit (Stratagene, La Jolla, CA) according to the manufacturer's protocol. The constructs were verified by DNA sequence analysis.

2.2. Cell culture

HEK293 cells (RIKEN Cell Bank, Tsukuba, Japan) were maintained in RPMI-1640 medium (Sigma, St. Louis, MO) supplemented with 10% fetal bovine serum (FBS) at 37 °C in a humidified atmosphere of 5% CO2. For the experiments, HEK293 cells were seeded in each well of 6-well plate at a density of 5×10^5 cells in 2 ml of 10% FBS-RPMI-1640 medium. After 12 h, each expression vector (2 μg) was transfected into HEK293 cells using FuGENE HD Transfection

Table 1
The sequences of primer sets for site-directed mutagenesis.

Primers	Sequences	
p.P123S	Forward	5′ GGATATGGTCTCTACTCTGCTTTTTTCTCCATCCTGACAT AC 3′
	Reverse	5′ GTATGTCAGGATGGAGAAAAAAGCAGAGTAGAGACCATATCC 3′
p.M147V	Forward	5′ CTTTTCCAGTGGTGAGTTTAGTGGTGGGATCTGTTGTTC 3′
	Reverse	5′ GAACAACAGATCCCACCACTAAACTCACCACTGGAAAAG 3′
p.K369E	Forward	5′ CTATTGCAGTGTCAGTAGGAGAAGTATATGCCACCAAGTATG 3′
	Reverse	5′ CATACTTGGTGGCATATACTTCTCCTACTGACACTGCAATAG 3′
p.A372V	Forward	5′ GTGTCAGTAGGAAAAGTATATGTCACCAAGTATGATTACACC 3′
	Reverse	5′ GGTGTAATCATACTTGGTGACATATACTTTTCCTACTGACAC 3′
p.N392Y	Forward	5′ GCCTTTGGGATCAGCTACATCTTCTCAGGATTCTTC 3′
	Reverse	5′ GAAGAATCCTGAGAAGATGTAGCTGATCCCAAAGGC 3′
p.C565Y	Forward	5′ CGATGGTTTTAAAAAATATATCAAGTCCACAGTTGGATTTGATGCC 3′
	Reverse	5′ GGCATCAAATCCAACTGTGGACTTGATATATTTTTTAAAACCATCG 3′
p.S657N	Forward	5′ CAAAGTGCCAATCCATAACCTTGTGCTTGACTGTG 3′
	Reverse	5′ CACAGTCAAGCACAAGGTTATGGATTGGCACTTTG 3′
p.S666F	Forward	5′ CTTGACTGTGGAGCTATATTTTTCCTGGACGTTGTTG 3′
	Reverse	5′ CAACAACGTCCAGGAAAAATATAGCTCCACAGTCAAG 3′
p.T721M	Forward	5′ CAACATTAGAAAGGACACATTCTTTTTGATGGTCCATGATGC 3′
	Reverse	5′ GCATCATGGACCATCAAAAAGAATGTGTCCTTTCTAATGTTG 3′
p.H723R	Forward	5′ CTTTTTGACGGTCCGTGATGCTATACTCTATCTACAG 3′
	Reverse	5′ C TGTAGATAGAGTATAGCATCACGGACCGTCAAAAAG 3′

Reagent (Roche, Grenzacherstrasse, Switzerland) according to the manufacturer's protocol. After transfection for 24–48 h, the cells were used for the following experiments.

2.3. Immunofluorescence microscopy

After incubation for 24 h of HEK293 cells transfected with each vector, the cells were replaced in 24-well glass bottom plates and further incubated for 24 h. Salicylate dissolved in distilled water was added to the cells in each well and the cells were incubated for 12 h in the presence of salicylate. For vehicle control, distilled water was added to the medium. The cells were washed 3 times with PBS and fixed with 4% paraformaldehyde for 5 min at room temperature. To avoid non-specific binding, the cells were incubated in blocking solution (50% Block Ace, Dainippon Sumitomo Pharma, Osaka, Japan and 50% FBS) for 1 h at 37 °C. After washing with PBS, the cells were incubated with mouse anti-FLAG primary antibody (Sigma) for 1 h at 37 °C and then anti-mouse IgG secondary antibody TRITC conjugated (Sigma) for 30 min at 37 °C. These antibodies were diluted in 0.1% (w/v) saponin-PBS. After washing with PBS, the fluorescence of cells stained with TRITC was observed using a confocal laser scanning microscope (FV500, Olympus, Tokyo, Japan).

To clarify where pendrin mutants are mainly expressed in the cells, fluorescence intensities of the cells were analyzed by FLUOVIEW (Olympus). As shown in Fig. 1, a green line was firstly drawn on the cell expressing wild-type pendrin, and intensities of TRITC and differential interference contrast (DIC) on the line were analyzed. Two peaks at the ends of the line in the TRITC intensity map and two low peaks in the DIC intensity map were detected. The two low peaks in the DIC intensity map showed the border between the cell and the glass of the culture plate. The width of the plasma membrane was determined to be 0.8 μm from the border, based on the width of the TRITC-related peaks in the TRITC intensity map. Then, the fluorescence intensities were obtained from the 20 regions (region size, 0.8 μm × 0.8 μm) of the plasma membrane area, and such intensities were also obtained from the 20 regions of the cytoplasm area. Each region was not overlapped and equally distributed from the cell center. The former and the latter regions covered approximately 90% and 70% of the plasma membrane area and the cytoplasm area, respectively. The ratio of the mean fluorescence intensities of the 20 regions obtained from the plasma membrane area to such intensities of the 20 regions obtained from the cytoplasm area was calculated. Finally, the main localization of each pendrin mutant was estimated by calculating the averaged ratio from the ratio obtained from 6 to 9 cells.

2.4. Iodide efflux assay

Iodide efflux from cells was assessed by a modification of the methods described by Gillam et al. (2004) and Dossena et al. (2006). After incubation for 36 h of HEK293 cells transfected with each vector, the cells in each well of the 6-well plate were incubated for 12 h at 37 °C in the medium in the presence or absence of salicylate. The cells were then incubated for 10 min at 37 °C in 1 ml of high Cl^- buffer (2 mM KCl, 135 mM NaCl, 1 mM CaCl2, 1 mM MgCl2, 10 mM D-glucose, 20 mM HEPES, pH7.4), and further incubated for 60 min at 37 °C in 1 ml of high I^- buffer (2 mM KCl, 135 mM NaI, 1 mM CaCl2, 1 mM MgCl2, 10 mM D-glucose, 20 mM HEPES, pH7.4) containing 200 kBq/ml ^{125}I. During these processes, uptake of ^{125}I is promoted by exchange with Cl^- already taken into the cells by a mechanism independent of pendrin. After washing with high I^- buffer, the cells were incubated for 10 min at 37 °C in 1 ml of high Cl^- buffer.

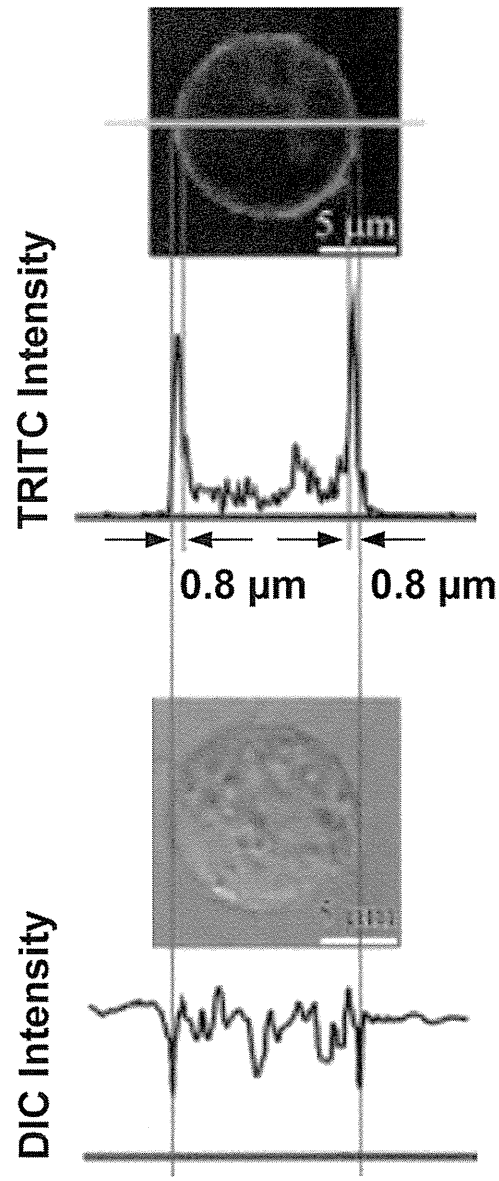

Fig. 1. Intensity analysis of intracellular localization of pendrin. A green line was drawn on the cell expressing wild-type pendrin, which mainly expresses in plasma membrane, and the intensities of TRITC and DIC on the line were analyzed. Two peaks at the ends of the line in the TRITC intensity map and the two low peaks in the DIC intensity map were detected. The two low peaks in the DIC intensity map showed the border between the cell and glass of the culture plate. The width of plasma membrane was determined to be 0.8 μm based on width of the TRITC-related peaks in the TRITC intensity map, and 0.8 μm inside from the border was defined the plasma membrane. (For interpretation of the references to colour in this figure legend, the reader is referred to the web version of this article.)

Replacement of high I^- buffer by high Cl^- buffer induces the export of ^{125}I from within cells to extracellular media by the activity of transfected pendrin. Finally, the cells were lysed in 200 μl of lysis buffer (0.1 M NaOH, 0.1% SDS, 2% sodium carbonate), and intracellular iodide content was determined by measuring radiolabeled-iodide in the cell lysates using a scintillation counter. The protein content in the lysates was measured by Bradford methods (Bio-Rad, Hercules, CA). Remaining radioactivity in cells was obtained by dividing intracellular iodide content in the lysates (cpm/ml) by protein content in the lysates (mg/ml).

2.5. Cytotoxicity assay

HEK293 cells cultured in each well of a 24-well glass bottom plate were incubated for 12 h at 37 °C in medium in the presence or absence (vehicle control) of 10 mM of salicylate. After incubation, nuclei in the cells were stained with 7-amino-actinomycin D (7-AAD, 200 ng/ml in medium) (Sigma) at 37 °C for 10 min. As 7-AAD penetrates plasma membranes of dying or dead cells but not viable cells, this compound is used as a marker for cell death. As a positive control, the plasma membrane of cells was permeated by incubation in methanol for 1 min and dried prior to the staining with 7-AAD. The fluorescence of the cells was observed by a confocal laser scanning microscope (Olympus).

2.6. Statistical analysis

The statistical significance of the results was analyzed using Dunnett's test for multiple comparisons and Student's *t*-test for unpaired observations.

3. Results

3.1. Expression of pendrin mutants in HEK293 cells

When wild-type pendrin was expressed in HEK293 cells, the fluorescence intensity of TRITC, which indicates localization of pendrin, was particularly strong on the plasma membrane compared with the fluorescence intensity of the empty vector transfected cells (Fig. 2). Two pendrin mutants, i.e., p.K369E and p.C565Y, were also localized on the plasma membrane (Fig. 2). On the other hand, other mutants, i.e., p.P123S, p.M147V, p.A372V, p.N392Y, p.S657N, p.S666F, p.T721M and p.H723R, were localized in the whole cell except for the regions of the nuclei (Fig. 2). These findings indicate that wild-type pendrin and two pendrin mutants, p.K369E and p.C565Y, were localized in the plasma membrane, whereas the other 8 pendrin mutants were retained in the cytoplasm.

3.2. Effects of salicylate on the localization of mutant pendrin

Eight pendrin mutants, i.e., p.P123S, p.M147V, p.A372V, p.N392Y, p.S657N, p.S666F, p.T721M and p.H723R, were retained in the cytoplasm of the HEK293 cells (Fig. 2). Therefore, we analyzed whether these 8 pendrin mutants are induced normal transport to the plasma membrane by salicylate. The 8 pendrin mutants were localized in cytoplasm when the cells were incubated in the absence of salicylate (Fig. 3a and c). In contrast, 10 mM of salicylate made the fluorescence intensity of TRITC of the plasma membrane stronger than that of the cytoplasm in the cells which expressed p.P123S, p.M147V, p.S657N and p.H723R (Fig. 3b and c). In this case, the fluorescence intensity of cytoplasm by TRITC becomes weaker and the nucleus and cytoplasm in the cell become unclear, because the pendrin mutants, i.e., p.P123S, p.M147V, p.S657N and p,H723R, translocate by the compound from the cytoplasm to the plasma membrane (Fig. 3b and c). As a result, the nucleus appears to be large (Fig. 3b). However, no changes were observed in the cells transfected with other mutants, i.e., p.A372V, p.N392Y, p.S666F and p.T721M (Fig. 3b and c). These findings indicate that salicylate induces the translocation of p.P123S, p.M147V, p.S657N and p.H723R pendrin mutants from the cytoplasm to the plasma membrane.

3.3. Effect of salicylate on the viability of HEK293 cells

To clarify whether 10 mM of salicylate has cytotoxicity, HEK293 cells were incubated for 12 h at 37 °C with or without 10 mM of salicylate, and the viability of cells was visualized by microscope. On treatment with salicylate, as well as vehicle control, no significant fluorescence intensity of 7-AAD binding to nuclei in the cells was observed (Fig. 4). In contrast, as a positive control, nuclei of the cells treated with methanol were clearly stained due to the increase in the permeability of the plasma membrane (Fig. 4). These findings indicate that 10 mM of salicylate has no cytotoxicity to HEK293 cells.

3.4. Effects of lower concentration of salicylate on the intracellular localization of p.P123S mutant pendrin

HEK293 cells expressing p.P123S pendrin mutant were incubated for 12 h in medium containing 1 or 10 mM of salicylate. The intracellular localization of the p.P123S pendrin mutant was detected by immunofluorescence microscopy. The p.P123S pendrin mutant was localized in plasma membrane when the cells were incubated in the presence of 10 mM of salicylate (Fig. 5). However, 1 mM of salicylate did not change the localization of p.P123S pendrin mutant when compared with vehicle control (Fig. 5). These findings indicate that salicylate at 10 mM but not at 1 mM induces the translocation of p.P123S mutant pendrin.

3.5. Effects of salicylate on the activity of pendrin

We analyzed whether the 4 pendrin mutants (p.P123S, p.M147V, p.S657N and p.H723R) translocated to the plasma membrane by salicylate act as transporters using radiolabeled-iodide. HEK293 cells transfected with the expression vector for the pendrin mutants were incubated with or without salicylate. In cells transfected with the wild-type pendrin expression vector, remaining radioactivity in cells was significantly decreased compared with that transfected with an empty vector when the cells were incubated in the absence of salicylate (Fig. 6). This finding indicates that wild-type pendrin has an activity to export iodide from cytoplasm. Remaining radioactivity in cells expressing the p.K369E or p.C565Y mutants, which were located in the plasma membrane as shown in Fig. 1, was decreased as in the case of wild-type pendrin (Fig. 6). Therefore, the mutants acted to transport iodide as do wild-type pendrin. In the expression of wild-type pendrin, the activity in the presence of 10 mM of salicylate was not significantly different from that in the absence of salicylate (Fig. 6), suggesting that the incubation with of 10 mM of salicylate does not affect the cellular condition and the wild-type pendrin activity. In case of transfection with 4 mutant pendrin genes encoding the mutants p.P123S, p.M147V, p.S657N and p.H723R, no significant change of remaining radioactivity in cells was observed compared with the empty control in the absence of salicylate treatment (Fig. 6). However, the remaining radioactivity in cells transfected with each mutant was significantly decreased by 10 mM of salicylate treatment (Fig. 6). These activities were almost the same as in the case of wild-type pendrin (Fig. 6). These findings indicate that salicylate restores pendrin activity.

4. Discussion

It is suggested that retention of some pendrin mutants in the endoplasmic reticulum is a major mechanism for Pendred syndrome (Rotman-Pikielny et al., 2002; Dossena et al., 2009). p.L236P, p.G384 and p.T416P pendrin mutants reported in Caucasians are accumulated in the endoplasmic reticulum and do not reach the plasma membrane due to their mutations (Rotman-Pikielny et al., 2002). In Japanese patients, 10 pendrin mutants, i.e., p.P123S, p.M147V, p.K369E, p.A372V, p.N392Y, p.C565Y, p.S657N, p.S666F, p.T721M and p.H723R, have been reported (Tsukamoto et al., 2003). Yoon et al. (2008) have reported that p.M147V and p.H723R pendrin mutants were accumulated in the endoplasmic reticulum due to their mutation. However,

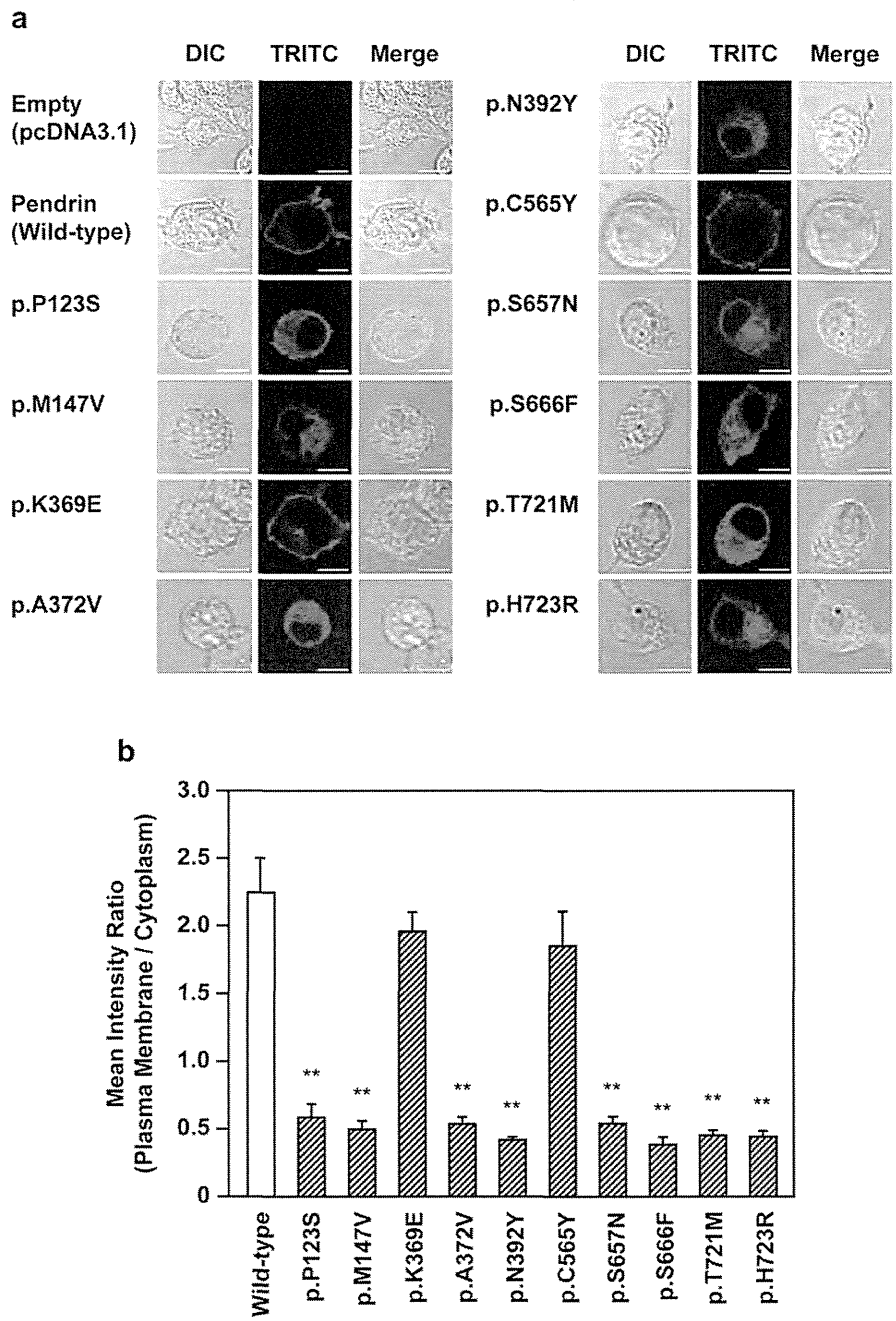

Fig. 2. Intracellular localization of pendrin and its mutants in HEK293 cells. HEK293 cells were transfected with the empty vector, the expression vector including wild-type pendrin gene or the mutant genes. (a) After 48 h, intracellular localization of pendrin was analyzed by immunofluorescent staining. The experiment shown is representative of 3 independent experiments. (b) The fluorescence intensities of the plasma membrane and cytoplasm of the cells were evaluated. The ratios were obtained by calculating the mean fluorescence intensities of 20 regions (0.8 μm × 0.8 μm) in plasma membrane and cytoplasm. Values are the means from 6 to 9 cells with SEM. $^{**}P < 0.01$ vs. wild-type. This figure shows that wild-type pendrin and two pendrin mutants p.K369E and p.C565Y were localized in the plasma membrane, whereas the other 8 pendrin mutants were retained in the cytoplasm. The bar indicates 10 μm.

intracellular localization and activity of 8 other pendrin mutants have remained to be elucidated. In this study, we demonstrated the following 4 points about the intracellular localization and activity of pendrin mutants reported in Japanese patients: (1) Among the 10 pendrin mutants reported in Japanese patients, p.K369E and p.C565Y are expressed in the plasma membrane of HEK293 cells, as is wild-type pendrin. (2) The other 8 mutants, i.e., p.P123S, p.M147V, p.A372V, p.N392Y, p.S657N, p.S666F, p.T721M and p.H723R, are accumulated in the cytoplasm of the cells. (3) In the 8 pendrin mutants retained in the cytoplasm of the cells, p.P123S, p.M147V, p.S657N and p.H723R are induced normal transport to the plasma membrane of the cells by 10 mM salicylate without cytotoxicity. (4) When induced normal transport to the plasma membrane by salicylate, these 4 pendrin mutants recovered their activity.

Pendrin is a member of the *SLC26A* gene family including prestin (Mount and Romero, 2004). In the inner ear, it is reported that the motor protein prestin plays an important role in hearing as the

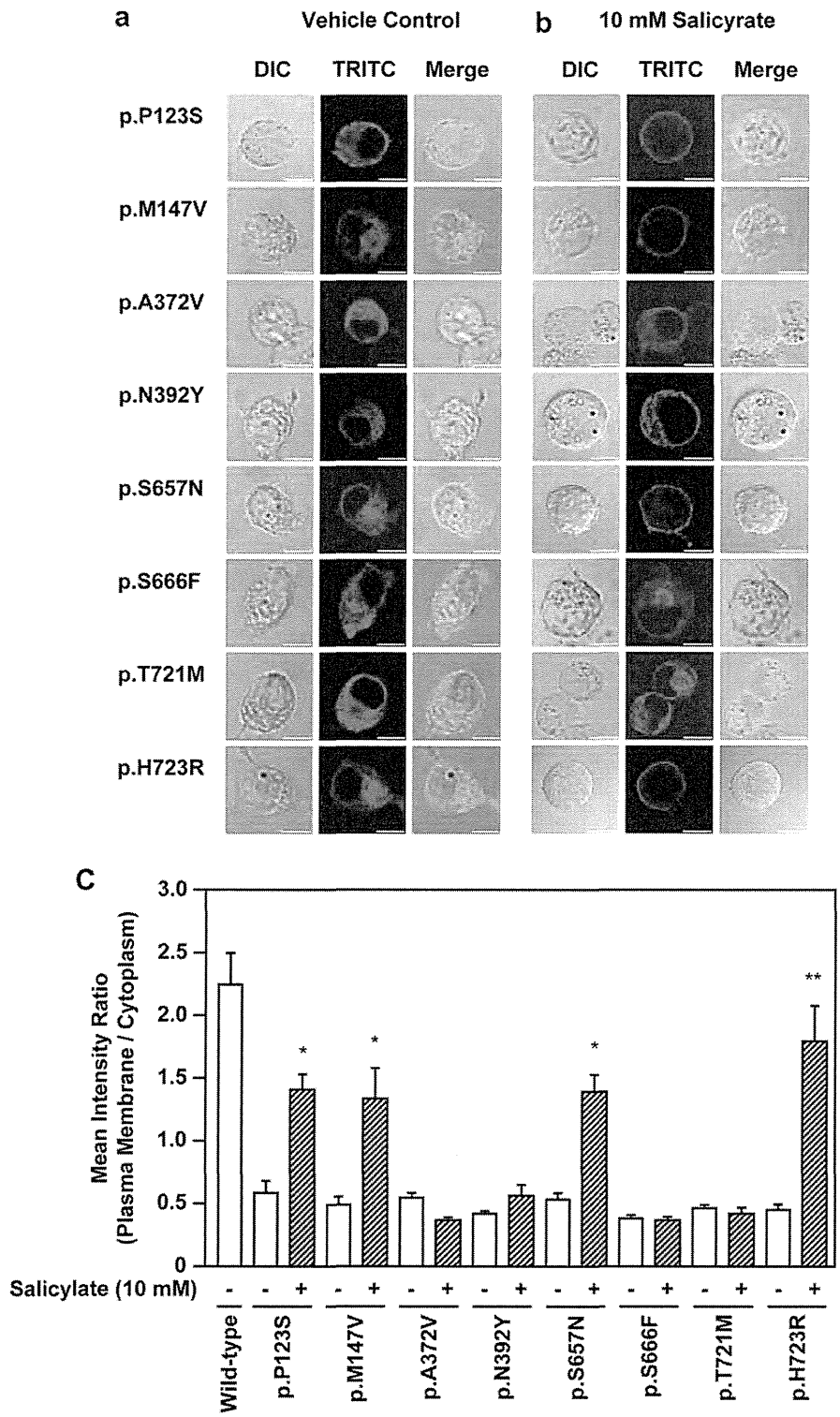

Fig. 3. Effects of salicylate on the intracellular localization of mutant pendrin. HEK293 cells were transfected with the expression vector including mutant pendrin gene. After 36 h, salicylate was added to the medium and the cells were further incubated for 12 h (a, b) Intracellular localization of pendrin was analyzed by immunofluorescent staining. The experiment shown is representative of 3 independent experiments. (c) The fluorescence intensities of the plasma membrane and cytoplasm of the cells were evaluated. The ratios were obtained by calculating the mean fluorescence intensities of 20 regions (0.8 μm × 0.8 μm) in plasma membrane and cytoplasm. Values are the means from 6 to 9 cells with SEM. $^{*}P < 0.05$, $^{**}P < 0.01$ vs. wild-type. This figure reveals that after incubation with salicylate, fluorescence intensity of TRITC of plasma membrane is stronger than that of the cytoplasm in the cells expressing p.P123S, p.M147V, p.S657N and p.H723R, but not in those expressing p.A372V, p.N392Y, p.S666F and p.T721M. The bar indicates 10 μm.

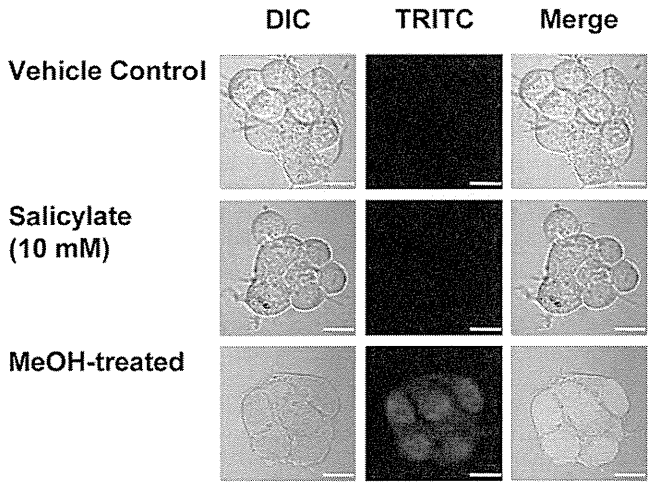

Fig. 4. Effects of salicylate on the viability of HEK293 cells. HEK293 cells were incubated for 12 h in medium containing 10% FBS in the presence or absence of 10 mM of salicylate. After incubation, the cells were stained with 7-AAD and observed by confocal microscopy. As a positive control, the membrane of cells incubated for 12 h in the absence of salicylate was permealyzed by methanol prior to the staining with 7-AAD. This figure indicates that 10 mM of salicylate has no cytotoxicity to HEK293 cells. The bar indicates 20 μm.

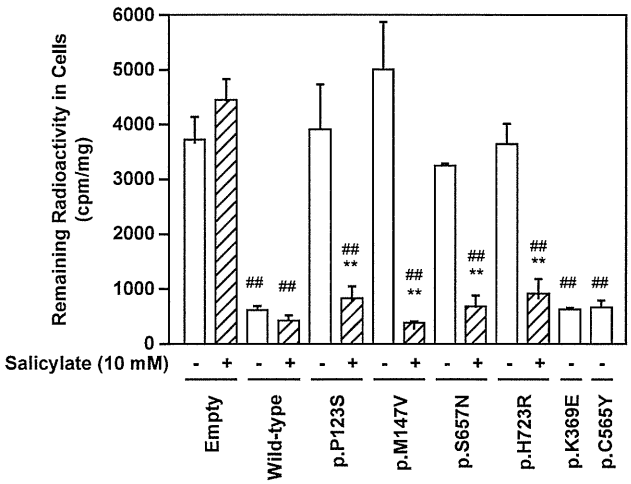

Fig. 6. Effects of salicylate on the iodide efflux from HEK293 cells. HEK293 cells were transfected with the empty vector, the expression vector including wild-type pendrin gene or the expression vector including the mutant genes. After 36 h, salicylate was added to the medium and the cells were further incubated for 12 h. The activity of pendrin was measured by radiolabeled-iodide efflux. The remaining radioactivity in cells was defined by dividing intracellular iodide content in the lysates (cpm/ml) by protein content in the lysates (mg/ml). This figure shows that the remaining radioactivity in the cells transfected with p.P123S, p.M147V, p.S657N and p.H723R was significantly decreased by salicylate. $**P < 0.01$ vs. corresponding control (the cells lacking salicylate), $\#\#P < 0.01$ vs. empty without salicylate.

origin of electromotility of the outer hair cells (Zheng et al., 2000). The nonlinear capacitance change involved in prestin requires some ions such as Cl^- and $HCO3^-$ and is inhibited by 10 mM of salicylate (Oliver et al., 2001). Recently, we have reported that salicylate induces the translocation of prestin mutants to the plasma membrane from the cytoplasm (Kumano et al., 2010). There is approximately a 45% similarity between pendrin and prestin in amino acid sequences and transport of anions by pendrin is similar to those transported by prestin (Mount and Romero, 2004). Therefore, we hypothesized that as is the case with prestin, salicylate modifies the function as a pharmacological chaperone for the pendrin mutants. As shown in Figs. 3 and 6, salicylate induced the transport of 4 pendrin mutants, i.e., p.P123S, p.M147V, p.S657N and p.H723R, to the plasma membrane and the recovery of their anion exchanger activity, while 4 other pendrin mutants, i.e., p.A372V, p.N392Y, p.S666F and p.T721M, were retained in the cytoplasm.

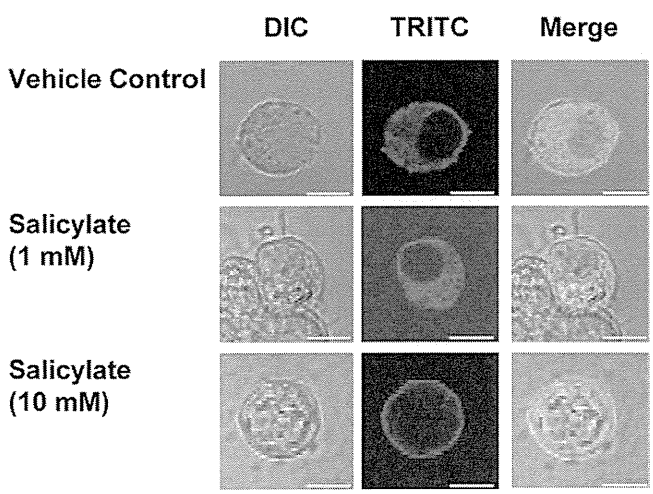

Fig. 5. Effects of lower concentration of salicylate on the intracellular localization of p.P123S mutant pendrin. HEK293 cells were transfected with the expression vector including p.P123S mutant pendrin. After 36 h, salicylate was added to the medium and the cells were further incubated for 12 h. Intracellular localization of pendrin was analyzed by immunofluorescent staining. This figure demonstrates that salicylate at 10 mM but not 1 mM induces the translocation of p.P123S mutant pendrin. The experiment shown is representative of 3 independent experiments. The bar indicates 10 μm.

Salicylate is a nonsteroidal anti-inflammatory drug (NSAID) which functions to inhibit cyclooxygenase-2 (COX-2) activity with an IC_{50} value of 14 μM (Cryer and Feldman, 1992; DuBois et al., 1996). Although salicylate at a concentration over 14 μM was expected to inhibit at least more than 50% of the COX-2 activity, in the present study, 1 mM salicylate did not induce the translocation of p.P123S pendrin mutants from the cytoplasm to the plasma membrane (Fig. 4). Therefore, it is unlikely that translocation of pendrin mutants to the plasma membrane by salicylate resulted from its COX2-inhibitory effect. Recently, it has been reported that salicylate also inhibits histone deacetylases (HDACs) at a concentration higher than that of COX-2 inhibition (DiRenzo et al., 2008). This might mean that inhibition of HDACs is one of the candidate mechanisms for the effect of salicylate on the translocation of pendrin mutants. Yoon et al. (2008) have reported that the p.H723R pendrin mutant is in the cytoplasm and is restored its location and $HCO3^-$ influx activity by 5 mM of sodium butyrate, which is an HDAC inhibitor (de Ruijter et al., 2003). HDACs are enzymes that remove the acetate from acetylated lysine residue in protein acetylated by histone acetyl transferases (HATs) (de Ruijter et al., 2003). Acetylation by HAT occurs in numerous proteins such as histone, transcription factors and heat shock proteins, and modifies their cellular functions (Ishihara et al., 2005). Therefore, hyperacetylated-proteins by the inhibition of HDACs induced by 10 mM of salicylate might lead to the translocation of pendrin mutants to the plasma membrane and recovery of their activity. In addition, it has been reported that glycosylation of pendrin effects its folding and ultimate localization (Yoon et al., 2008; Rebeh et al., 2009). Therefore, it is necessary to analyze the involvement of pendrin acetylation and glycosylation on the translocation and recovery of the activity of the pendrin mutants by 10 mM of salicylate.

In this study, we found that 4 mutants, i.e., p.P123S, p.M147V, p.S657N and p.H723R, were induced normal transport from the intracellular region and that they were restored their activity by

10 mM of salicylate, while 4 other mutants, i.e., p.A372V, p.N392Y, p.S666F and p.T721M, were not induced normal transport and were not restored their activity (Figs. 2 and 5). We confirmed that there was no significant difference in the protein levels of expression of wild-type pendrin and 10 pendrin mutants by Western blotting. Therefore, the recovery of the activity of 4 pendrin mutants, i.e., p.P123S, p.M147V, p.S657N and p.H723R, is considered to be due to the alterations in localization rather than to the level of protein expression. It has been reported that p.H723R pendrin mutant is mostly expressed in the endoplasmic reticulum, whereas p.L236P pendrin mutant is in the centrosomal region of the cells (Yoon et al., 2008). In that report, p.H723R but not p.L236P interestingly was restored its $HCO3^-$ influx activity by sodium butyrate. Therefore, it is possible that intracellular localization of pendrin mutants (p.P123S, p.M147V, p.S657N and p.H723R) targeted to the plasma membrane by salicylate differs from that of 4 other pendrin mutants (p.A372V, p.N392Y, p.S666F and p.T721M). Clarification of the mechanism by which salicylate induces the translocation of pendrin mutants is important and requires further study.

In this study, we showed that p.K369E and p.C565Y were expressed in the plasma membrane (Fig. 1) and acted to export iodide (Fig. 5), although pendrin genes with mutations in p.K369E and p.C565Y have been recognized as candidate genes in Japanese patients with NSEVA (Tsukamoto et al., 2003). It has been shown that p.S166N found in Korean patients was expressed in the plasma membrane with Cl^-/HCO_3^- exchange activity (Yoon et al., 2008). Recently, p.C565Y pendrin mutant has also been reported to be expressed on the plasma membrane, and the exchange activities for ions such as chloride and bicarbonate were reduced in comparison to wild-type pendrin but greater than the functional null control

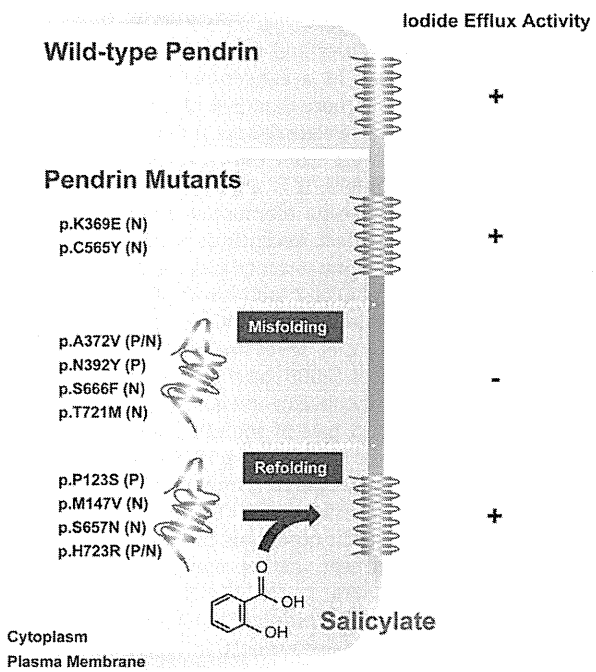

Fig. 7. Summary of pendrin mutants and *in vitro* effects of salicylate. Wild-type pendrin and two pendrin mutants, i.e., p.K369E and p.C565Y, are correctly folded, transported to the plasma membrane from the cytoplasm, and act to export iodide. In contrast, the other 8 pendrin mutants, i.e., p.P123S, p.M147V, p.A372V, p.N392Y, p.S657N, p.S666F, p.T721M and p.H723R, are retained in the cytoplasm. In the 8 pendrin mutants retained in the cytoplasm, 4 pendrin mutants, i.e., p.P123S, p.M147V, p.S657N and p.H723R, are translocated by salicylate to the plasma membrane, where the functions of 4 pendrin mutants are restored. The phenotypes (Pendred syndrome:P, NSEVA: N) related to the mutations reported by Tsukamoto et al. (2003) are represented.

(Choi et al., 2009). Thus, the relationship between those three mutations and NSEVA is unclear. As those three mutations were identified as compound heterozygous with other mutations in the pendrin gene (Tsukamoto et al., 2003; Park et al., 2004), it may be possible that NSEVA occurred when p.K369E, p.C565Y and p.S166N pendrin mutants were expressed with other pendrin mutants in the same cells. Further investigation is necessary to clarify how p.K369E and p.C565Y pendrin mutants are involved in NSEVA.

Pendred syndrome is characterized by sensorineural hearing impairment, presence of goiter, and a partial defect in iodide organification (Kopp et al., 2008). In the thyroid gland, pendrin releases iodide at the apical membrane of thyroid follicular cells into the follicular lumen to synthesize thyroid hormones, T3 and T4 (Kopp et al., 2008). Impairment of this function by pendrin mutants causes goiter and a partial defect in iodide organification. We have shown, in this study, that salicylate restores the iodide efflux activity of 4 pendrin mutants, i.e., p.P123S, p.M147V, p.S657N and p.H723R (Fig. 6), suggesting that salicylate restores the function in the thyroid. Although it is necessary to analyze the exchange activity for chloride and bicarbonate in the inner ear, salicylate could improve the condition of people suffering from Pendred syndrome caused by the mutation of p.P123S, p.M147V, p.S657N and p.H723R.

5. Conclusion

In conclusion, this is the report describing the intracellular localization of reported Japanese pendrin mutants. Of 10 pendrin mutants, 2 mutants and wild-type pendrin were found to be located in the plasma membrane, while 8 mutants were retained in the cytoplasm. Furthermore, we demonstrated that the function of 4 pendrin mutants was restored by salicylate (Fig. 7). This finding suggests that salicylate is a potentially promising compound for treatment of hearing loss that is associated with defects in protein localization, including a subset of individuals with Pendred syndrome. Our findings could contribute to further investigation for understanding disorders involving pendrin mutants.

Acknowledgements

This work was supported by Grant-in-Aid for Scientific Research on Priority Areas 15086202 from the Ministry of Education, Culture, Sports, Science and Technology of Japan, by Grant-in-Aid for Scientific Research (B) 20390439 from the Japan Society for the Promotion of Science, by Grant-in-Aid for Exploratory Research 20659263 from the Ministry of Education, Culture, Sports, Science and Technology of Japan, by a grant from the Human Frontier Science Program, by a Health and Labor Science Research Grant from the Ministry of Health, Labor and Welfare of Japan, by a grant from the Iketani Science and Technology Foundation, by a grant from the Daiwa Securities Health Foundation and by Tohoku University Global COE Program "Global Nano-Biomedical Engineering Education and Research Network Centre" to H.W.

References

Choi, B.Y., Stewart, A.K., Madeo, A.C., Pryor, S.P., Lenhard, S., Kittles, R., Eisenman, D., Kim, H.J., Niparko, J., Thomsen, J., Arnos, K.S., Nance, W.E., King, K.A., Zalewski, C.K., Brewer, C.C., Shawker, T., Reynolds, J.C., Butman, J.A., Karniski, L.P., Alper, S.L., Griffith, A.J., 2009. Hypo-functional SLC26A4 variants associated with nonsyndromic hearing loss and enlargement of the vestibular aqueduct: genotype–phenotype correlation or coincidental polymorphisms? Hum. Mutat. 30, 599–608.

Cryer, B., Feldman, M., 1992. Effects of nonsteroidal anti-inflammatory drugs on endogenous gastrointestinal prostaglandins and therapeutic strategies for prevention and treatment of nonsteroidal anti-inflammatory drug-induced damage. Arch. Intern. Med. 152, 1145–1155.

Conn, P.M., Leaños-Miranda, A., Janovick, J.A., 2002. Protein origami: therapeutic rescue of misfolded gene products. Mol. Interv. 2, 308–316.

de Ruijter, A.J., van Gennip, A.H., Caron, H.N., Kemp, S., van Kuilenburg, A.B., 2003. Histone deacetylases (HDACs): characterization of the classical HDAC family. Biochem. J. 370, 737–749.

DiRenzo, F., Cappelletti, G., Broccia, M.L., Giavini, E., Menegola, E., 2008. The inhibition of embryonic histone deacetylases as the possible mechanism accounting for axial skeletal malformations induced by sodium salicylate. Toxicol. Sci. 104, 397–404.

Dossena, S., Rodighiero, S., Vezzoli, V., Bazzini, C., Sironi, C., Meyer, G., Fürst, J., Ritter, M., Garavaglia, M.L., Fugazzola, L., Persani, L., Zorowka, P., Storelli, C., Beck-Peccoz, P., Bottá, G., Paulmichl, M., 2006. Fast fluorometric method for measuring pendrin (SLC26A4) Cl^-/I^- transport activity. Cell. Physiol. Biochem. 18, 67–74.

Dossena, S., Rodighiero, S., Vezzoli, V., Nofziger, C., Salvioni, E., Boccazzi, M., Grabmayer, E., Bottà, G., Meyer, G., Fugazzola, L., Beck-Peccoz, P., Paulmichl, M., 2009. Functional characterization of wild-type and mutated pendrin (SLC26A4), the anion transporter involved in Pendred syndrome. J. Mol. Endocrinol. 43, 93–103.

DuBois, R.N., Giardiello, F.M., Smalley, W.E., 1996. Nonsteroidal anti-inflammatory drugs, eicosanoids, and colorectal cancer prevention. Gastroenterol. Clin. North. Am. 25, 773–791.

Everett, L.A., Glaser, B., Beck, J.C., Idol, J.R., Buchs, A., Heyman, M., Adawi, F., Hazani, E., Nassir, E., Baxevanis, A.D., Sheffield, V.C., Green, E.D., 1997. Pendred syndrome is caused by mutations in a putative sulphate transporter gene (PDS). Nat. Genet. 17, 411–422.

Gillam, M.P., Sidhaye, A.R., Lee, E.J., Rutishauser, J., Stephan, C.W., Kopp, P., 2004. Functional characterization of pendrin in a polarized cell system. Evidence for pendrin-mediated apical iodide efflux. J. Biol. Chem. 279, 13004–13010.

Ishihara, K., Hong, J., Zee, O., Ohuchi, K., 2005. Mechanism of the eosinophilic differentiation of HL-60 clone 15 cells induced by n-butyrate. Int. Arch. Allergy Immunol. 137 (Suppl. 1), 77–82.

Janovick, J.A., Maya-Nunez, G., Conn, P.M., 2002. Rescue of hypogonadotropic hypogonadism-causing and manufactured GnRH receptor mutants by a specific protein-folding template: misrouted proteins as a novel disease etiology and therapeutic target. J. Clin. Endocrinol. Metab. 87, 3255–3262.

Kakehata, S., Santos-Sacchi, J., 1996. Effects of salicylate and lanthanides on outer hair cell motility and associated gating charge. J. Neurosci. 16, 4881–4889.

Kopp, P., 1999. Pendred's syndrome: clinical characteristics and molecular basis. Curr. Opin. Endocrinol. Diabetes 6, 261–269.

Kopp, P., Pesce, L., Solis-S, J.C., 2008. Pendred syndrome and iodide transport in the thyroid. Trends Endocrinol. Metab. 19, 260–268.

Kumano, S., Iida, K., Ishihara, K., Murakoshi, M., Tsumoto, K., Ikeda, K., Kumagai, I., Kobayashi, T., Wada, H., 2010. Salicylate-induced translocation of prestin having mutation in the GTSRH sequence to the plasma membrane. FEBS Lett. 584, 2327–2332.

Loo, T.W., Clarke, D.M., 1997. Correction of defective protein kinesis of human P-glycoprotein mutants by substrates and modulators. J. Biol. Chem. 272, 709–712.

Morello, J.P., Salahpour, A., Laperrière, A., Bernier, V., Arthus, M.F., Lonergan, M., Petäjä-Repo, U., Angers, S., Morin, D., Bichet, D.G., Bouvier, M., 2000. Pharmacological chaperones rescue cell-surface expression and function of misfolded V2 vasopressin receptor mutants. J. Clin. Invest. 105, 887–895.

Mount, D.B., Romero, M.F., 2004. SLC26 gene family of multifunctional anion exchangers. Pflugers Arch. 447, 710–721.

Oliver, D., He, D.Z., Klöcker, N., Ludwig, J., Schulte, U., Waldegger, S., Ruppersberg, J.P., Dallos, P., Fakler, B., 2001. Intracellular anions as the voltage sensor of prestin, the outer hair cell motor protein. Science 292, 2340–2343.

Park, H.J., Lee, S.J., Jin, H.S., Lee, J.O., Go, S.H., Jang, H.S., Moon, S.K., Lee, S.C., Chun, Y.M., Lee, H.K., Choi, J.Y., Jung, S.C., Griffith, A.J., Koo, S.K., 2004. Genetic basis of hearing loss associated with enlarged vestibular aqueducts in Koreans. Clin. Genet. 67, 160–165.

Rebeh, I.B., Yoshimi, N., Hadj-Kacem, H., Yanohco, S., Hammami, B., Mnif, M., Araki, M., Ghorbel, A., Ayadi, H., Masmoudi, S., Miyazaki, H., 2009. Two missense mutations in SLC26A4 gene: a molecular and functional study. Clin. Genet. 78, 74–80.

Rotman-Pikielny, P., Hirschberg, K., Maruvada, P., Suzuki, K., Royaux, I.E., Green, E.D., Kohn, L.D., Lippincott-Schwartz, J., Yen, P.M., 2002. Retention of pendrin in the endoplasmic reticulum is a major mechanism for Pendred syndrome. Hum. Mol. Genet. 11, 2625–2633.

Royaux, I.E., Wall, S.M., Karniski, L.P., Everett, L.A., Suzuki, K., Knepper, M.A., Green, E.D., 2001. Pendrin, encoded by the Pendred syndrome gene, resides in the apical region of renal intercalated cells and mediates bicarbonate secretion. Proc. Natl. Acad. Sci. USA 98, 4221–4226.

Scott, D.A., Wang, R., Kreman, T.M., Sheffield, V.C., Karniski, L.P., 1999. The Pendred syndrome gene encodes a chloride–iodide transport protein. Nat. Genet. 21, 440–443.

Taubes, G., 1996. Misfolding the way to disease. Science 271, 1493–1495.

Thomas, P.J., Qu, B.H., Pedersen, P.L., 1995. Defective protein folding as a basis of human disease. Trends Biochem. Sci. 20, 456–459.

Tsukamoto, K., Suzuki, H., Harada, D., Namba, A., Abe, S., Usami, S., 2003. Distribution and frequencies of PDS (SLC26A4) mutations in Pendred syndrome and nonsyndromic hearing loss associated with enlarged vestibular aqueduct: a unique spectrum of mutations in Japanese. Eur. J. Hum. Genet. 11, 916–922.

Tunstall, M.J., Gale, J.E., Ashmore, J.F., 1995. Action of salicylate on membrane capacitance of outer hair cells from the guinea-pig cochlea. J. Physiol. 485, 739–752.

Ulloa-Aguirre, A., Janovick, J.A., Brothers, S.P., Conn, P.M., 2004. Pharmacologic rescue of conformationally-defective proteins: implications for the treatment of human disease. Traffic 5, 821–837.

Wangemann, P., Nakaya, K., Wu, T., Maganti, R.J., Itza, E.M., Sanneman, J.D., Harbidge, D.G., Billings, S., Marcus, D.C., 2007. Loss of cochlear $HCO3^-$ secretion causes deafness via endolymphatic acidification and inhibition of Ca^{2+} reabsorption in a Pendred syndrome mouse model. Am. J. Physiol. Renal Physiol. 292, F1345–F1353.

Welch, W.J., Brown, C.R., 1996. Influence of molecular and chemical chaperones on protein folding. Cell Stress Chaperones 1, 109–115.

Yoon, J.S., Park, H.J., Yoo, S.Y., Namkung, W., Jo, M.J., Koo, S.K., Park, H.Y., Lee, W.S., Kim, K.H., Lee, M.G., 2008. Heterogeneity in the processing defect of SLC26A4 mutants. J. Med. Genet. 45, 411–419.

Yoshino, T., Sato, E., Nakashima, T., Nagashima, W., Teranishi, M.A., Nakayama, A., Mori, N., Murakami, H., Funahashi, H., Imai, T., 2004. The immunohistochemical analysis of pendrin in the mouse inner ear. Hear. Res. 195, 9–16.

Zheng, J., Shen, W., He, D.Z., Long, K.B., Madison, L.D., Dallos, P., 2000. Prestin is the motor protein of cochlear outer hair cells. Nature 405, 149–155.

FEBS Letters 584 (2010) 2872–2876

FEBS Letters

journal homepage: www.FEBSLetters.org

Atomic force microscopy imaging of the structure of the motor protein prestin reconstituted into an artificial lipid bilayer

Shun Kumano, Michio Murakoshi, Koji Iida, Hiroshi Hamana, Hiroshi Wada *

Department of Bioengineering and Robotics, Tohoku University, 6-6-01 Aoba-yama, Sendai 980-8579, Japan

ARTICLE INFO

Article history:
Received 2 March 2010
Revised 29 April 2010
Accepted 30 April 2010
Available online 7 May 2010

Edited by Sandro Sonnino

Keywords:
Prestin
Membrane protein
Atomic force microscopy
Outer hair cell
Inner ear

ABSTRACT

Prestin is the motor protein of cochlear outer hair cells and is essential for mammalian hearing. The present study aimed to clarify the structure of prestin by atomic force microscopy (AFM). Prestin was purified from Chinese hamster ovary cells which had been modified to stably express prestin, and then reconstituted into an artificial lipid bilayer. Immunofluorescence staining with anti-prestin antibody showed that the cytoplasmic side of prestin was possibly face up in the reconstituted lipid bilayer. AFM observation indicated that the cytoplasmic surface of prestin was ring-like with a diameter of about 11 nm.

1. Introduction

The basis of electromotility of outer hair cells (OHCs) which realizes the high sensitivity of mammalian hearing is considered to be the motor protein prestin [1]. Several characteristics of prestin have been gradually clarified [2]. Murakoshi et al. [3] detected prestin in the plasma membrane of prestin-transfected Chinese hamster ovary (CHO) cells using Qdots as topographic markers and observed ring-like structures, possibly prestin, by atomic force microscopy (AFM). Mio et al. [4] observed prestin purified from prestin-transfected insect cells by transmission electron microscopy (TEM) and found prestin to be a bullet-shaped molecule. Although those two studies are significant, their observed images differed, indicating that the structure of prestin was unclear. Thus, the aim of the present study was to clarify such structure by reconstitution of purified prestin into an artificial lipid bilayer and observation of the prestin-reconstituted lipid bilayer by AFM.

2. Materials and methods

2.1. Purification of prestin

The purification of prestin was performed by the method established in our previous study with some modifications [5]. CHO cells which had been modified to stably express C-terminal 3×FLAG-tagged prestin were suspended in Tris–KCl buffer (10 mM Tris, 150 mM KCl, pH 7.4) and sonicated, followed by centrifugation at 1000×*g* for 7 min at 4 °C to remove nuclei and undisrupted cells. The obtained supernatant was centrifuged at 20360×*g* at 4 °C for 2 h to collect the membrane fraction of the cells. Membrane proteins were solubilized by resuspending the obtained membrane fraction in Tris–KCl buffer containing 10 mM *n*-nonyl-β-D-thiomaltopyranoside (NTM, Dojindo, Kumamoto, Japan). After 3-h incubation on ice, samples were centrifuged at 20360×*g* at 4 °C for 3 h to remove non-solubilized proteins. The supernatant was applied to a column filled with anti-FLAG affinity gel (Sigma–Aldrich, St. Louis, MO). The column was then washed with Tris–KCl buffer containing 0.065 mM Fos-Cholin-16 (Anatrace, Maumee, OH) to replace the detergent NTM with Fos-Choline-16. Afterward, prestin was competitively eluted with 1 ml of that buffer containing 500 μg/ml of 3×FLAG peptide (Sigma–Aldrich). Whether prestin was purified or not was confirmed by SDS–PAGE, followed by Western blotting with anti-FLAG antibody and HRP-conjugated anti-mouse IgG antibody and by silver staining.

Abbreviations: OHC, outer hair cell; CHO, Chinese hamster ovary; AFM, atomic force microscopy; TEM, transmission electron microscopy

* Corresponding author. Hiroshi Wada, Department of Bioengineering and Robotics, Tohoku University, 6-6-01 Aoba-yama, Sendai 980-8579, Japan. Fax: +81 22 795 6939.
E-mail address: wada@cc.mech.tohoku.ac.jp (H. Wada).

0014-5793/$36.00
doi:10.1016/j.febslet.2010.04.076

2.2. Reconstitution of prestin into a preformed lipid bilayer

The method of direct reconstitution of membrane proteins into a preformed lipid bilayer was applied in the present study [6]. An artificial lipid bilayer was formed on mica using dioeoyl-phosphatidylcholine (DOPC) and dipalmitoyl-phosphatidylcholine (DPPC) (Avanti Polar Lipids, Alabaster, AL). The lipid bilayer was preincubated for 30 min at 4 °C with Tris–KCl buffer containing 5 mM $CaCl_2$ and 0.0065 mM Fos-cholin-16 for equilibration of the detergent within the lipid bilayer. Afterward, such bilayer was incubated with Tris–KCl buffer containing purified prestin, 5 mM $CaCl_2$ and 0.039 mM Fos-cholin-16 for 15 min at 4 °C. Excess prestin was then removed by extensive rinsing with Tris–KCl buffer. As a negative control, the lipid bilayer treated with detergent but without prestin was also prepared.

2.3. Staining of prestin in the reconstituted lipid bilayer

The existence of prestin in the lipid bilayer was confirmed by immunofluorescence staining. The prestin-reconstituted lipid bilayer was incubated with Block Ace (Dainippon Pharmaceutical Co. Osaka, Japan) for 30 min at 37 °C to avoid non-specific binding of antibodies. Afterward, that bilayer was stained with goat anti-prestin N-terminus primary antibody (Santa Cruz Biotechnology, Santa Cruz, CA, USA) at a dilution of 1:100 in PBS overnight at 4 °C and with anti-goat IgG Texas Red (Santa Cruz Biotechnology) at a dilution of 1:200 in PBS at 37 °C for 60 min. The stained lipid bilayer was observed by confocal microscopy.

2.4. AFM imaging

The height images of the lipid bilayer were acquired in Tris–KCl buffer filtered with a 0.2-μm nylon filter by Multimode V AFM with a Nanoscope V controller (Veeco, Santa Barbara, CA) at 24–26 °C. V-shaped Si_3N_4 cantilevers (OMCL-TR400PSA-2, Olympus, Tokyo, Japan) with a spring constant of 0.06 N/m were used. The AFM was operated in the oscillation imaging mode (Tapping mode™, Digital Instruments) at a scan frequency of 1–0.5 kHz. In the present study, three types of images were obtained by AFM, namely, low- (5.0 × 5.0 μm), middle- (1.0 × 1.0 μm) and high-magnification images (300 × 300 nm). Each scan line has 256 and 512 points of data and an image consists of 256 and 512 scan lines for low magnification images and for middle- and high-magnification images, respectively. Obtained AFM images were flattened by use of a software program (NanoScope v7.00, Veeco) to eliminate background slopes and to correct dispersions of individual scanning lines. In addition, only high-magnification images were low-pass filtered to reduce high frequency noise. When the observed structure was ring-like, the distance between two peaks based on the cross sections was taken to be its diameter, as was done in our previous study [3].

3. Results

3.1. Purification of prestin

Whether prestin was indeed purified or not was investigated by SDS–PAGE, followed by Western blotting and silver staining. Results of Western blotting and silver staining are shown in Fig. 1A and B, respectively. In the Western blotting image, the 100 kDa band, probably showing prestin, was detected. In the results of silver staining, only one band corresponding to the band observed in Western blotting was recognized.

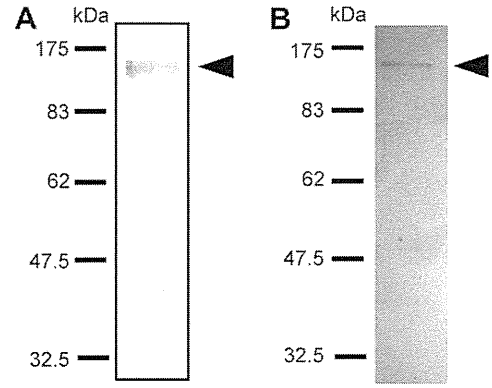

Fig. 1. Results of Western blotting and silver staining. (A) Western blotting data. A 100 kDa band probably showing prestin is seen. (B) Result of silver staining of SDS–PAGE gel. Only one band at 100 kDa, which was thought to correspond to the band detected in the result of Western blotting, is recognized.

3.2. Immunofluorescence staining of the prestin-reconstituted lipid bilayer

After the reconstitution process, immunofluorescence staining was employed to investigate whether prestin had been incorporated into the preformed lipid bilayer. Representative immunofluorescence images of the prestin-reconstituted lipid bilayer and negative control sample are shown in Fig. 2. Red fluorescence was detected in the prestin-reconstituted lipid bilayer but not in the negative control sample.

3.3. AFM imaging of the lipid bilayer

The AFM height image of the lipid bilayer without treatment showed two kinds of flat domains (Fig. 3A). A similar image was also obtained from the negative control sample (Fig. 3B). Unlike those two images, in addition to the flat domain, bumpy domains indicated by white arrows were detected in the low magnification AFM image of the prestin-reconstituted lipid bilayer (Fig. 3C). The boxed area in Fig. 3C was scanned by AFM and the obtained image is depicted in Fig. 3D. Dense small particles, some of which were recognized as ring-like structures, can be observed in that image. To clearly visualize the observed particles, the boxed area in Fig. 3D was scanned by AFM, the acquired image being shown in Fig. 3E. Moreover, three-dimensional representation of Fig. 3E is depicted in Fig. 4. Many ring-like structures were confirmed to be densely embedded in the lipid bilayer. The average diameter of such structures in Fig. 3E and other AFM images which are not shown here is 11.0 ± 1.3 nm ($n = 42$).

4. Discussion

4.1. Reconstitution of prestin into an artificial lipid bilayer

After the purification process, only the 100 kDa band corresponding to the band in Western blotting data was detected by silver staining of SDS–PAGE gel, indicating that prestin had been purified. The 100 kDa band probably shows the monomer of prestin. As SDS possibly affects the binding between prestin molecules, to clearly confirm the oligomerization of purified prestin, a mild detergent such as perfluoro-octanoic acid should be used as in the study by Zheng et al. [7]. The AFM height image of the lipid bilayer without treatment shows two types of flat domains (Fig. 3A), as seen in previous studies [6,8–11]. At 24–26 °C, DOPC forms fluid-phase domains, while DPPC forms gel-phase domains. The thickness of DPPC in the gel-phase is larger than that of DOPC in

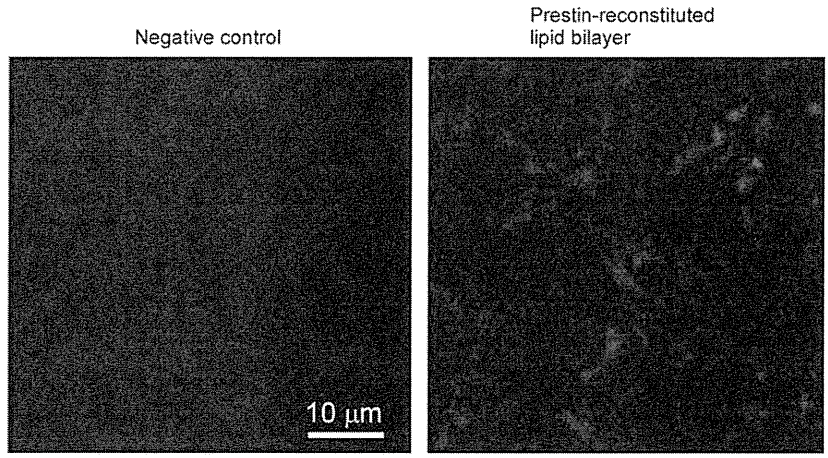

Fig. 2. Immunofluorescence staining of prestin-reconstituted lipid bilayer. Negative control sample and the prestin-reconstituted lipid bilayer were stained with anti-prestin antibody and anti-goat IgG Texas Red. Red fluorescence indicating the existence of prestin is only found in the prestin-reconstituted lipid bilayer.

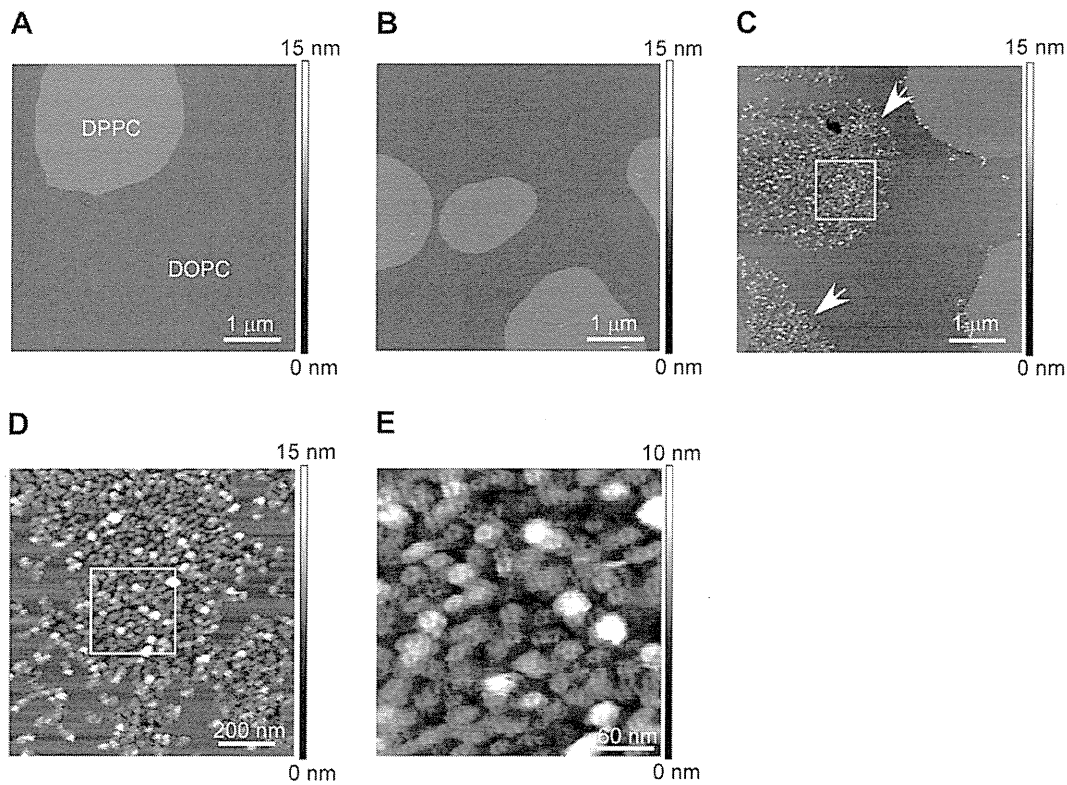

Fig. 3. AFM height images of the lipid bilayer. (A) AFM image of the lipid bilayer without treatment at low magnification. (B) AFM image of the negative control sample at low magnification. (C) AFM image of prestin-reconstituted lipid bilayer at low magnification. (D) Middle-magnification image obtained by scanning of the boxed area shown in (C). (E) High-magnification image obtained by scanning of the boxed area shown in (D). Two kinds of flat domains in (A) and (B) probably represent the domain of DPPC in the gel-phase and that of DOPC in the fluid-phase. Bumpy domains indicated by white arrows can be detected in the prestin-reconstituted lipid bilayer shown in (C). Many small particles can be found in the middle-magnification AFM images and those particles were recognized as ring-like in the high-magnification image. Such ring-like structures probably show prestin molecules.

the fluid-phase, thus indicating that the two types of observed domains were due to the difference in the thickness between the two lipids. After the reconstitution process, immunofluorescence staining using anti-prestin antibody showed that prestin existed in the reconstituted lipid bilayer (Fig. 2). In the AFM image, the bumpy domains, which probably corresponded to prestin, were recognized only in DOPC domains of the prestin-reconstituted lipid bilayer. Milhiet et al. [6] have also suggested that proteins of interest were reconstituted only into the DOPC domains in the fluid state. Thus, the present study and their study imply that proteins tend to be reconstituted into the DOPC domains in the fluid state. In the AFM image at high-magnification, ring-like structures probably showing prestin were densely reconstituted into the lipid bilayer. However, the alignment of such structures as found in the OHC plasma membrane by Sinha et al. [12] was not detected, which might have resulted from differences in the environment

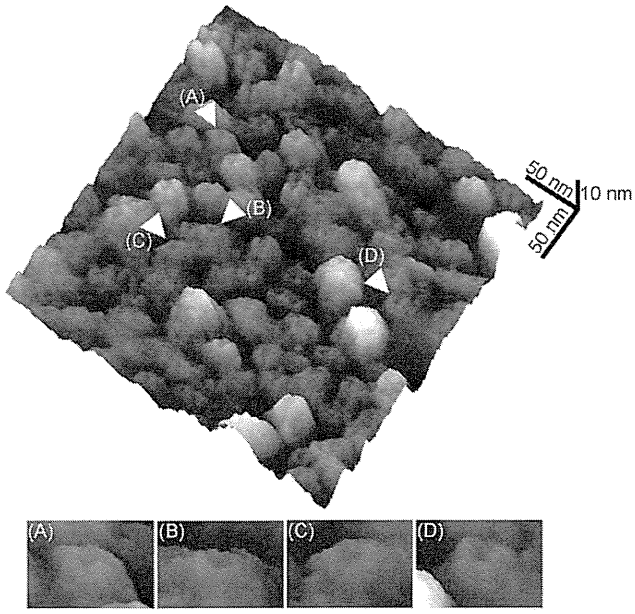

Fig. 4. Three-dimensional AFM height image of the prestin-reconstituted lipid bilayer. This figure was created from Fig. 3E. Representative examples of ring-like structures were digitally magnified and are shown (A and B). Ring-like structures, considered to be similar to those observed in the study of Murakoshi et al. [3], are found to be densely embedded in the lipid bilayer.

Table 1
Comparison of the size of prestin.

Sample	Method	Diameter (nm)	References
OHC plasma membrane	AFM	11–25	Le Grimellec et al. [15]
Purified prestin	TEM	7.7–9.6	Mio et al. [4]
Prestin-expressing CHO cell plasma membrane	AFM	9.6/13.0	Murakoshi et al. [3]
OHC plasma membrane	AFM	10	Sinha et al. [12]
Prestin-reconstituted lipid bilayer	AFM	11.0 ± 1.3	This study

between the OHC plasma membrane and the artificial lipid bilayer. The existence of actin cytoskeleton in OHCs and that of mica in the present study would affect the alignment of prestin.

4.2. Orientation of prestin

The orientation of prestin should be considered to confirm which side of prestin was observed by AFM, the extracellular side or the cytoplasmic side. Previous reports have suggested that when membrane proteins were reconstituted into a preformed lipid bilayer as done in the present study, their unidirectional orientation was obtained [6,13,14], indicating that all prestin molecules reconstituted into the lipid bilayer might be oriented in the same direction. In the present study, the standard deviation of the diameter of the observed ring-like structure, 1.3 nm, was small. Small standard deviation might increase the possibility that only either prestin molecules whose extracellular side was exposed or such molecules whose cytoplasmic side was exposed existed in the reconstituted lipid bilayer. Data showed in the previous reports, small standard deviation of the diameter and successful staining of such bilayer with anti-prestin antibody which binds to the cytoplasmic side of prestin possibly implied that the cytoplasmic side of prestin was face up. Although the possibility that the extracellular side of a few prestin molecules was exposed was not completely ruled out, it was considered that AFM possibly visualized the cytoplasmic side of prestin in the present study.

4.3. Structure and size of prestin

The AFM image of the prestin-reconstituted lipid bilayer showed dense ring-like structures, each with a diameter of 11.0 ± 1.3 nm, which were probably the surface structure of the cytoplasmic side of prestin. The previously reported sizes of prestin obtained by observation of the cytoplasmic side of prestin are listed in Table 1 [3,4,12,15]. Although it is unclear whether the particles detected in OHC plasma membranes are only comprised of prestin or not, our result is consistent with the previously reported sizes, supporting the assumption that the observed structures were prestin.

Le Grimellec et al. [15] found structures with a central depression in the cytoplasmic side of the OHC plasma membrane by AFM. Murakoshi et al. [3] showed by AFM that prestin might form a ring-like structure. On the other hand, Mio et al. [4] suggested that prestin is a bullet-shaped molecule which protrudes into the cytoplasmic side. Although Sinha et al. [12] found 10-nm particles in the cytoplasmic side of the OHC plasma membrane by AFM, whether those particles were ring-like or not was not specified. Thus, the structure of prestin has been a controversial issue. Our results demonstrate that prestin may form a ring-like structure with a diameter of about 11 nm, which agrees with results of Le Grimellec et al. [15] and Murakoshi et al. [3].

In summary, the present study attempted to visualize prestin purified and reconstituted into the artificial lipid bilayer by AFM. From the obtained AFM image, the cytoplasmic surface of prestin was indicated to be ring-like with a diameter of about 11 nm.

Acknowledgements

This work was supported by Grant-in-Aid for Scientific Research on Priority Areas 15086202 from the Ministry of Education, Culture, Sports, Science and Technology of Japan, by Grant-in-Aid for Scientific Research (B) 18390455 from the Japan Society for the Promotion of Science, by Grant-in-Aid for Exploratory Research 18659495 from the Ministry of Education, Culture, Sports, Science and Technology of Japan, by a grant from the Human Frontier Science Program, by a Health and Labour Science Research Grant from the Ministry of Health, Labour and Welfare of Japan, and by Tohoku University Global COE Program "Global Nano-Biomedical Engineering Education and Research Network Centre" to H.W., and by a Grant-in-Aid for JSPS Fellows from the Japan Society for the Promotion of Science to S.K.

References

[1] Zheng, J., Shen, W., He, D.Z.Z., Long, K.B., Madison, L.D. and Dallos, P. (2000) Prestin is the motor protein of cochlear outer hair cells. Nature 405, 149–155.
[2] Ashmore, J. (2008) Cochlear outer hair cell. Physiol. Rev. 88, 173–210.
[3] Murakoshi, M., Iida, K., Kumano, S. and Wada, H. (2009) Immune atomic force microscopy of prestin-transfected CHO cells using quantum dots. Pflugers Arch. 457, 885–898.
[4] Mio, K., Kubo, Y., Ogura, T., Yamamoto, T., Arisaka, F. and Sato, C. (2008) The motor protein prestin is a bullet-shaped molecule with inner cavities. J. Biol. Chem. 283, 1137–1145.
[5] Iida, K., Murakoshi, M., Kumano, S., Tsumoto, K., Ikeda, K., Kobayashi, T., Kumagai, I. and Wada, H. (2008) Purification of the motor protein prestin from Chinese hamster ovary cells stably expressing prestin. JBSE 3, 221–234.
[6] Milhiet, P.E., Gubellini, F., Berquand, A., Dosset, P., Rigaud, J.L., Le Grimellec, C. and Levy, D. (2006) High-resolution AFM of membrane proteins directly incorporated at high density in planar lipid bilayer. Biophys. J. 91, 3268–3275.
[7] Zheng, J., Du, G.G., Anderson, C.T., Keller, J.P., Orem, A., Dallos, P. and Cheatham, M. (2006) Analysis of the oligomeric structure of the motorprotein prestin. J. Biol. Chem. 281, 19916–19924.
[8] Morandat, S. and Kirat, K.E. (2006) Membrane resistance to Triton X-100 explored by real-time atomic force microscopy. Langmuir 22, 5786–5791.

[9] Berquand, A., Levy, D., Gubellini, F., Le Grimellec, C. and Milhiet, P. (2007) Influence of calcium on direct incorporation of membrane proteins into in-plane lipid bilayer. Ultramicroscopy 107, 928–933.
[10] Francius, G., Dufour, S., Deleu, M., Paquot, M., Mingeot-Leclercq, M. and Dufrêne, Y.E. (2008) Nanoscale membrane activity of surfactins: influence of geometry, charge and hydrophobicity. Biochim. Biophys. Acta 1778, 2058–2068.
[11] Mingeot-Leclercq, M., Deleu, M., Brasseur, R. and Dufrêne, Y.F. (2008) Atomic force microscopy of supported lipid bilayers. Nat. Protoc. 3, 1654–1659.
[12] Sinha, G.P., Sabri, F., Dimitriadis, E.K. and Iwasa, K.H. (2010) Organization of membrane motor in outer hair cells: an atomic force microscopic study. Pflugers Arch. 459, 427–439.
[13] Rigaud, J., Paternostre, M. and Bluzat, A. (1988) Mechanism of membrane protein insertion into liposomes during reconstitution procedures involving the use of detergents. 2. Incorporation of the light-driven proton pump bacteriorhodopsin. Biochemistry 27, 2677–2688.
[14] Rigaud, J., Pitard, B. and Levy, D. (1995) Reconstitution of membrane proteins into liposome: application to energy-transducing membrane proteins. Biochim. Biophys. Acta 1231, 223–246.
[15] Le Grimellec, C., Giocondi, M.C., Lenoir, M., Vater, M., Sposito, G. and Pujol, R. (2002) High-resolution three-dimensional imaging of the lateral plasma membrane of cochlear outer hair cells by atomic force microscopy. J. Comp. Neurol. 451, 62–69.

FEBS Letters 584 (2010) 2327–2332

journal homepage: www.FEBSLetters.org

Salicylate-induced translocation of prestin having mutation in the GTSRH sequence to the plasma membrane

Shun Kumano [a], Koji Iida [a], Kenji Ishihara [a], Michio Murakoshi [a], Kouhei Tsumoto [b], Katsuhisa Ikeda [c], Izumi Kumagai [d], Toshimitsu Kobayashi [e], Hiroshi Wada [a,*]

[a] Department of Bioengineering and Robotics, Tohoku University, Sendai, Japan
[b] Department of Medical Genome Sciences, The University of Tokyo, Kashiwa, Japan
[c] Department of Otorhinolaryngology, Juntendo University School of Medicine, Tokyo, Japan
[d] Department of Biomolecular Engineering, Tohoku University, Sendai, Japan
[e] Department of Otolaryngology, Head and Neck Surgery, Tohoku University Graduate School of Medicine, Sendai, Japan

ARTICLE INFO

Article history:
Received 14 February 2010
Revised 24 March 2010
Accepted 7 April 2010
Available online 11 April 2010

Edited by Gianni Cesareni

Keywords:
Prestin
Motor protein
Mutation
Salicylate
Outer hair cell
Inner ear

ABSTRACT

Prestin is a key molecule for mammalian hearing. The present study investigated changes in characteristics of prestin by culturing prestin-transfected cells with salicylate, an antagonist of prestin. As a result, the plasma membrane localization of prestin bearing a mutation in the GTSRH sequence, which normally accumulates in the cytoplasm, was recovered. Moreover, the nonlinear capacitance of the majority of the mutants, which is a signature of prestin activity, was also recovered. Thus, the present study discovered a new effect of salicylate on prestin, namely, the promotion of the plasma membrane expression of prestin mutants in an active state.

1. Introduction

The motor protein prestin in the plasma membrane of cochlear outer hair cells (OHCs) is believed to be the origin of their electromotility [1]. So far, several characteristics of prestin have been clarified by introduction of mutations into prestin [2]. Mutations in membrane proteins sometimes cause the accumulation of these proteins in the cytoplasm. It has been reported that when the cells expressing such accumulated mutants were cultured with a pharmacological chaperone, which is a cell membrane-permeable molecule with high affinity for these mutants, the chaperone bound to them and promoted their transport to the plasma membrane in an active state [3–7]. Salicylate, which is known as an antagonist of prestin, is thought to have cell membrane permeability with high affinity for prestin [8,9]. Thus, salicylate was considered to be a candidate molecule to work as a pharmacological chaperone for prestin. In the present study, the aim was to investigate whether or not salicylate has the ability to promote the plasma membrane expression of prestin mutants accumulated in the cytoplasm.

2. Materials and methods

2.1. Prestin mutants

Our previous study showed that mutations in the GTSRH sequence at positions 127–131 of prestin caused a decrease in nonlinear capacitance (NLC), which is a signature of prestin activity [10]. Such decrease may be due to the accumulation of prestin in the cytoplasm. Thus, the present study used the prestin mutants created in our previous study, namely, G127A, T128A, S129A, R130A, H131A and S129T. These mutants were engineered to be expressed in HEK293 cells by transfection. As the prestin genes were co-transfected with green fluorescent protein (GFP) gene into the cells, transfected cells were selected by GFP observation.

Abbreviations: OHC, outer hair cell; NLC, nonlinear capacitance; GFP, green fluorescent protein; WT, wild-type; WGA, wheat germ agglutinin

* Corresponding author at: Address: Department of Bioengineering and Robotics, Tohoku University, 6-6-01 Aoba-yama, Sendai 980-8579, Japan. Fax: +81 22 795 6939.
E-mail address: wada@cc.mech.tohoku.ac.jp (H. Wada).

0014-5793/$36.00 © 2010 Federation of European Biochemical Societies. Published by Elsevier B.V. All rights reserved.
doi:10.1016/j.febslet.2010.04.010

2.2. Incubation of transfected cells with salicylate

Transfected cells were cultured with salicylate, which is generally known to have the ability to suppress NLC as an antagonist of prestin, to confirm another effect of salicylate as a pharmacological chaperon for prestin. It was reported that, in the patch-clamp recording, 10 mM salicylate around the cells was required for almost complete suppression of NLC, which might be realized by the binding of salicylate with prestin in the plasma membrane [9]. Thus, for the binding of salicylate with prestin, at least 10 mM salicylate was considered to be necessary. Although salicylate possibly affects the cell viability, it has been reported that more than 85% of HEK293 cells were able to survive in the presence of up to 10 mM sodium salicylate [11]. In the present study, the cells were cultured for 24-36 hours in growth medium with sodium salicylate at a concentration of 10 mM from 12 hours after transfection. After such incubation, the cells were used in experiments. The cells cultured without salicylate were employed as control samples. Samples of the cells expressing wild-type (WT) prestin and its mutants which were cultured with 10 mM salicylate were termed WT prestin+Sal, G127A+Sal, T128A+Sal, S129A+Sal, R130A+Sal, H131A+Sal and S129T+Sal.

2.3. Confirmation of the localization of prestin in transfected cells

The localization of prestin in the cells was assessed by immunofluorescence staining with anti-FLAG antibody, TRITC-conjugated anti-mouse IgG antibody and wheat germ agglutinin (WGA)-Alexa Fluor 633 conjugate as described in our previous study [12]. In the present study, several tens of transfected cells were observed for

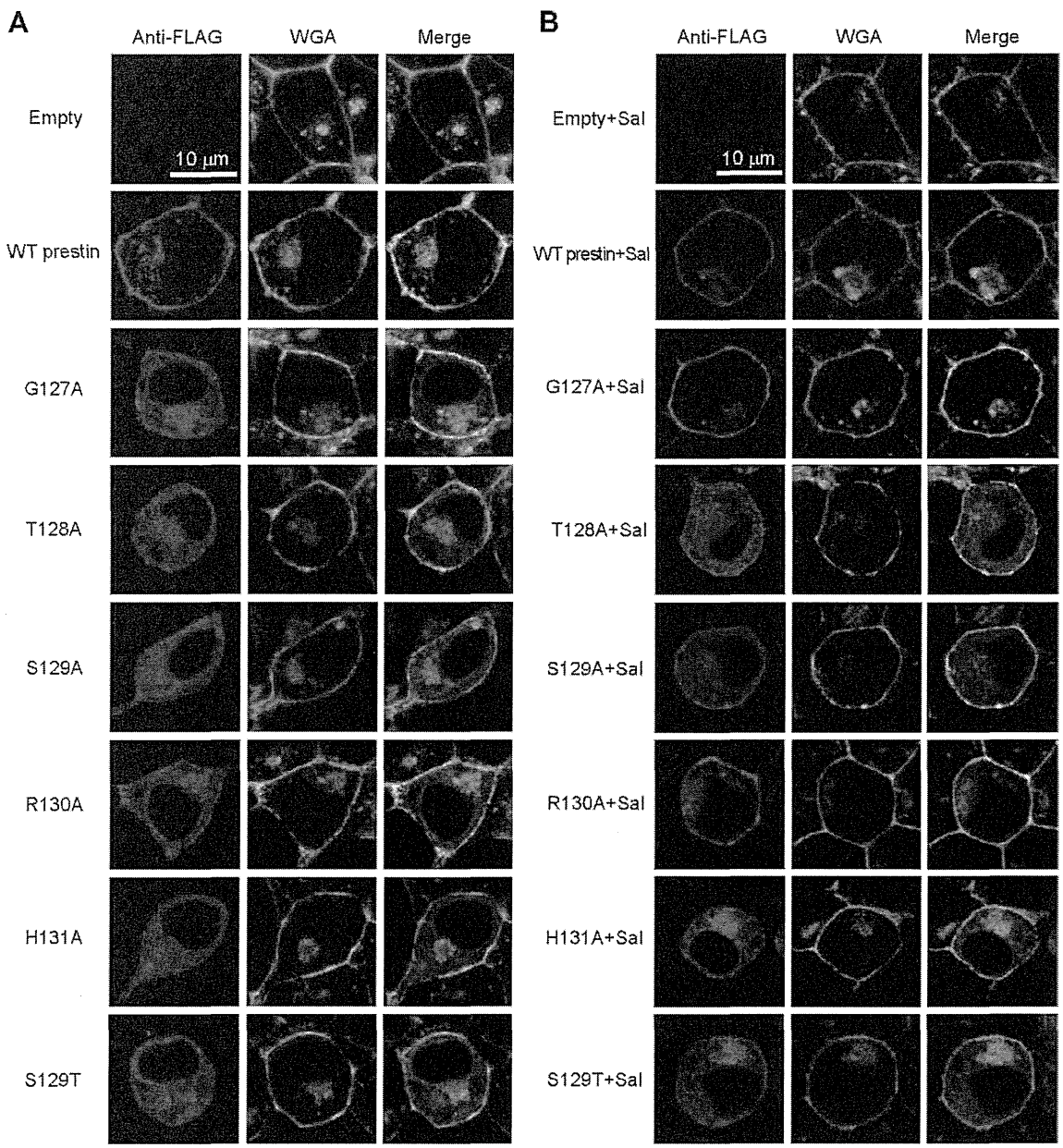

Fig. 1. Representative immunofluorescence images of transfected cells. (A) Stained cells cultured without 10 mM salicylate. (B) Stained cells cultured with 10 mM salicylate. Red and green fluorescence show prestin and both the plasma membrane and Golgi bodies, respectively. In the merged images, yellow–orange fluorescence indicates the co-localization of prestin and the plasma membrane, and that of prestin and the Golgi bodies.

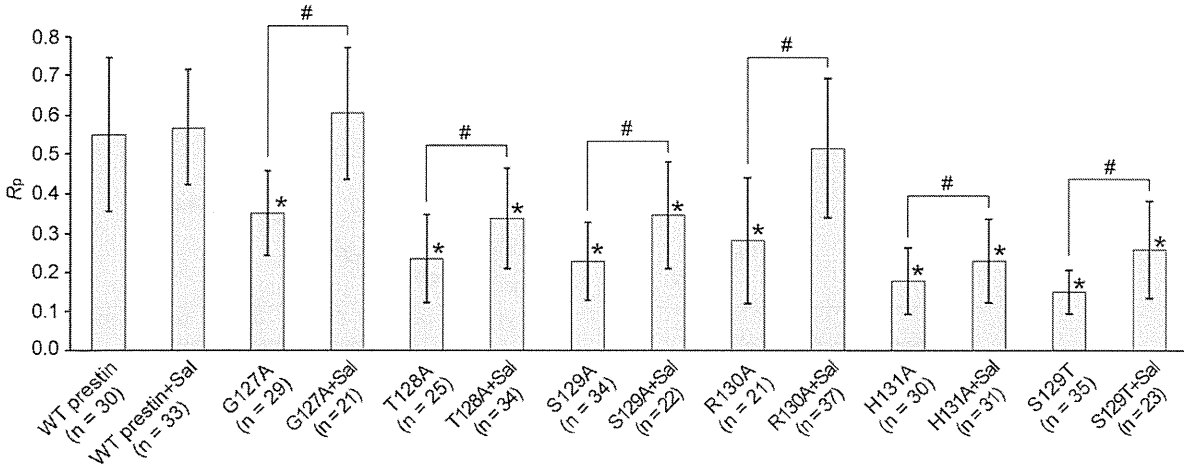

Fig. 2. R_p of WT prestin and its mutants. The R_p values of all prestin mutants were statistically lower than that of WT prestin when salicylate was not used, but they were increased by 10 mM salicylate. Asterisks show the statistical differences in the R_p values between WT prestin and the prestin mutants and between WT prestin+Sal and the prestin mutants+Sal ($p < 0.05$). Number signs indicate statistical differences between R_p values obtained from cells cultured with salicylate and those obtained from cells cultured without it in each prestin mutant ($p < 0.05$). Error bars show standard deviations.

each prestin mutant and the ratio of the amount of prestin in the plasma membrane to the total amount of prestin in the cell, R_p, was investigated. R_p was calculated by the following equation:

$$R_p = \frac{I_p}{I_w}, \tag{1}$$

where I_w is the sum of the intensity values of TRITC fluorescence of the whole area of the target cell which reflects the total amount of prestin in the cell, and I_p is the sum of the intensity values of TRITC fluorescence of only the pixels corresponding to the plasma membrane, which reflects the amount of prestin there. The I_w and I_p were calculated as described in our previous study [12].

2.4. Evaluation of electrophysiological properties of prestin

NLC, which is generally used for the analysis of prestin activity, was measured in the whole-cell patch-clamp recording as described in our previous study [13]. Transfected cells were washed just before the recording. By such washing, salicylate bound to prestin in the plasma membrane was expected to be dissociated [9]. The cells without membrane disruption which showed robust GFP fluorescence were selected for measurement. The recorded membrane capacitance was fitted with the first derivative of the Boltzmann function [14],

$$C_m(V) = C_{lin} + \frac{Q_{max}}{\alpha e^{\frac{V-V_{1/2}}{\alpha}}\left(1+e^{-\frac{V-V_{1/2}}{\alpha}}\right)^2}, \tag{2}$$

where C_{lin} is the linear capacitance, which is proportional to the membrane area of the cells, Q_{max} is the maximum charge transfer, V is the membrane potential and $V_{1/2}$ is the voltage at half-maximal charge transfer. In Eq. (2), α is the slope factor of the voltage-dependent charge transfer and is given by

$$\alpha = kT/ze, \tag{3}$$

where k is Boltzmann's constant, T is absolute temperature, z is valence and e is electron charge. To evaluate the maximum charge transfer of prestin in the unit plasma membrane, Q_{max}, which means the maximum charge transfer of prestin in whole plasma membrane, was divided by C_{lin} and designated as charge density.

For the comparison of NLC curve, NLC had to be normalized by the area of the plasma membrane. The normalized NLC $C_{nonlin/lin}$ was defined as

$$C_{nonlin/lin}(V) = \frac{C_{nonlin}}{C_{lin}} = \frac{(C_m(V) - C_{lin})}{C_{lin}}, \tag{4}$$

where C_{nonlin} is the nonlinear component of the measured membrane capacitance.

2.5. Concentration dependence of effects of salicylate on prestin

The relationship between the concentration of salicylate and the degree of the promotion of the plasma membrane expression of prestin mutants was investigated. The cells transfected with R130A were cultured with sodium salicylate at concentrations of 1 mM and 5 mM from 12 h after transfection. By the above-mentioned method, after 24 h of incubation, the cells were subjected to immunofluorescence staining and the R_p was then calculated.

3. Results and discussion

3.1. Localization of prestin in transfected cells

Representative immunofluorescence images of stained cells which were cultured without and with 10 mM salicylate are shown in Fig. 1A and B, respectively. To statistically investigate the localization of prestin in the cells, the R_p was calculated and shown in Fig. 2. Without salicylate, the R_p values of the prestin mutants were statistically lower than that of WT prestin ($p < 0.05$), suggesting that those mutants were accumulated in the cytoplasm. To confirm whether or not salicylate has the ability to promote the plasma membrane expression of the prestin mutants, prestin-transfected cells were cultured with 10 mM salicylate. The R_p of WT prestin was unchanged by 10 mM salicylate, indicating that such amount of salicylate did not affect the process of transport of WT prestin to the plasma membrane (Fig. 2). On the other hand, the R_p values of all prestin mutants statistically increased, compared with those when salicylate was not used ($p < 0.05$). Especially, the R_p of G127A+Sal and that of R130A+Sal were similar to that of WT prestin+Sal. These results indicate that salicylate promoted the plasma membrane expression of the prestin mutants accumulated in the cytoplasm.

3.2. Electrophysiological properties of prestin

The $C_{nonlin/lin}$ (V), and charge density and α of WT prestin and its mutants are shown in Figs. 3 and 4, respectively. Without